

Supplementary Information

Influence of polymerisation conditions on the kinetics of poly(lactic-*co*-glycolic acid)-*b*-poly(ethylene glycol)-*b*-poly(lactic-*co*-glycolic acid) triblock synthesis and the occurrence of transesterification side reactions

Jie Yan, Paula Facal Marina, Anton Blencowe*

Applied Chemistry and Translational Biomaterials (ACTB) Group, Centre for Pharmaceutical Innovation (CPI), Clinical and Health Sciences, University of South Australia, Adelaide, South Australia 5001, Australia

Supporting Tables

Table S1. Conversion of L and G, and molecular weight characteristics of PLGA-PEG-PLGA copolymers at different time points for thermal polymerizations (PEG:L:G = 1:20:5, $[L]_0 = 3.42$ M, $[G]_0 = 0.85$ M).

Temp (°C)	Time (h)	Lactide conv. (%) ^a	Glycolide conv. (%) ^a	Total monomer conv. (%)	L/G mol conv. ratio	$M_{n,NMR}$ (kDa) ^a	$M_{n,GPC}$ (kDa) ^b	$M_{w,GPC}$ (kDa) ^b	PDI ^b
100	0.25	2.0	6.7	4.3	1.18	1.6	2.1	2.2	1.08
	1	3.8	20.0	11.9	0.77	1.7	2.1	2.3	1.08
	2	6.5	26.7	16.6	0.98	1.8	2.2	2.4	1.08
	4	11.5	53.3	32.4	0.86	2.1	2.4	2.6	1.08
	6	16.0	64.7	40.3	0.99	2.3	2.5	2.7	1.08
	8	16.7	68.8	42.7	0.97	2.4	2.5	2.7	1.08
	10	18.0	75.0	46.5	0.96	2.5	2.5	2.8	1.09
	24	31.1	94.0	63.1	1.30	2.9	2.7	3.0	1.11
	48	45.7	98.9	72.3	1.85	3.4	3.0	3.4	1.13
	72	58.8	99.7	79.3	2.36	3.8	3.1	3.5	1.15
96	78.2	> 99.9	89.1	3.13	4.3	2.9	3.6	1.24	
110	0.25	2.0	7.1	4.6	1.10	1.6	2.1	2.3	1.07
	1	4.8	23.1	13.9	0.83	1.8	2.3	2.4	1.07
	2	9.1	42.9	26.0	0.85	2.0	2.5	2.7	1.08
	4	14.5	62.5	38.5	0.93	2.3	2.7	2.9	1.07
	6	18.7	75.0	46.8	1.00	2.5	2.8	3.0	1.08
	24	50.7	99.1	74.9	2.05	3.5	3.2	3.6	1.11
	48	82.8	> 99.9	91.4	3.31	4.5	3.5	4.0	1.14
	72	90.4	> 99.9	95.2	3.61	4.7	3.4	4.0	1.18
120	0.25	2.0	13.3	7.6	0.59	1.6	2.1	2.3	1.07
	1	7.4	38.5	22.9	0.77	1.9	2.4	2.6	1.08
	2	13.8	56.3	35.0	0.98	2.2	2.7	2.9	1.07
	4	20.6	78.9	49.8	1.05	2.6	3.0	3.2	1.07
	6	27.0	90.0	58.5	1.20	2.8	3.1	3.4	1.09
	24	67.5	99.6	83.6	2.71	4.0	3.6	4.0	1.12
	48	90.0	> 99.9	95.0	3.60	4.7	3.7	4.3	1.16

^a Calculated via ¹H NMR spectroscopy. ^b Calculated via GPC against narrow molecular weight PEG calibrants.

Table S2. Conversion of L and G, and molecular weight characteristics of PLGA-PEG-PLGA copolymers at different time points for the Sn(Oct)₂ catalysed polymerisation at different catalyst loadings (PEG:L:G = 1:20:5, [L]₀ = 3.42 M, [G]₀ = 0.85 M, 100 °C).

Catalyst loading (wt%)	Time (h)	Lactide conv. (%) ^a	Glycolide conv. (%) ^a	Total monomer conv. (%)	L/G mol conv. ratio	$M_{n,NMR}$ (kDa) ^a	$M_{n,GPC}$ (kDa) ^b	$M_{w,GPC}$ (kDa) ^b	PDI ^b
0.1	0.25	3.0	13.3	8.2	0.91	1.7	2.1	2.2	1.08
	1	5.9	41.2	23.5	0.57	1.9	2.4	2.6	1.07
	2	11.1	55.6	33.3	0.80	2.1	2.5	2.7	1.07
	6	17.9	81.0	49.5	0.89	2.5	2.9	3.1	1.08
	8	20.5	82.6	51.6	0.99	2.6	2.8	3.0	1.10
	10	22.0	87.0	54.5	1.01	2.6	2.6	2.9	1.11
	24	48.4	97.8	73.1	1.98	3.5	2.4	3.0	1.21
0.2	0.25	4.8	7.1	6.0	2.67	1.7	2.0	2.2	1.08
	1	12.3	40.0	26.1	1.23	2.1	2.3	2.5	1.08
	2	16.0	52.9	34.5	1.21	2.3	2.4	2.6	1.08
	4	21.3	68.4	44.8	1.24	2.5	2.4	2.7	1.15
	6	27.5	81.0	54.2	1.36	2.8	2.5	2.9	1.16
	8	30.6	86.4	58.5	1.42	2.9	2.5	2.9	1.17
	10	34.2	87.5	60.9	1.56	3.0	2.6	3.0	1.18
24	58.7	97.6	78.1	2.40	3.8	2.7	3.3	1.23	
0.4	0.25	3.8	6.7	5.3	2.31	1.6	2.3	2.5	1.07
	1	12.3	37.5	24.9	1.31	2.1	2.6	2.8	1.07
	2	17.4	55.6	36.5	1.25	2.3	3.0	3.1	1.06
	4	24.2	70.0	47.1	1.39	2.6	2.9	3.1	1.07
	6	30.1	81.8	55.9	1.47	2.8	3.0	3.3	1.07
	8	32.4	86.4	59.4	1.50	2.9	3.0	3.3	1.11
	10	36.7	88.0	62.4	1.67	3.1	2.6	3.2	1.22
24	62.4	97.9	80.1	2.55	3.9	3.0	3.6	1.22	

^a Calculated via ¹H NMR spectroscopy. ^b Calculated *via* GPC against narrow molecular weight PEG calibrants.

Table S3. Conversion of L and G, and molecular weight characteristics of PLGA-PEG-PLGA copolymers at different time points for the Sn(OTf)₂ catalysed polymerisation at different catalyst loadings (PEG:L:G = 1:20:5, [L]₀ = 3.42 M, [G]₀ = 0.85 M, 100 °C).

Catalyst loading (wt%)	Time (h)	Lactide conv. (%) ^a	Glycolide conv. (%) ^a	Total monomer conv. (%)	L/G mol conv. ratio	<i>M_{n,NMR}</i> (kDa) ^a	<i>M_{n,GPC}</i> (kDa) ^b	<i>M_{w,GPC}</i> (kDa) ^b	PDI ^b
0.1	0.25	2.0	6.7	4.3	1.18	1.6	1.5	1.6	1.05
	1	9.1	21.4	15.3	1.70	1.9	1.7	1.8	1.07
	2	13.0	26.7	19.9	1.96	2.0	1.7	1.8	1.08
	4	18.7	47.1	32.9	1.59	2.3	1.6	1.8	1.12
	6	23.1	61.1	42.1	1.51	2.5	1.6	1.9	1.14
	8	29.1	68.2	48.6	1.71	2.7	1.6	1.9	1.15
	24	58.3	95.3	76.8	2.45	3.7	1.7	2.0	1.17
0.4	0.25	2.9	15.4	9.1	0.76	1.7	1.8	2.0	1.09
	1	25.9	73.7	49.8	1.41	2.7	1.7	2.1	1.20
	2	42.5	88.9	65.7	1.91	3.2	1.9	2.2	1.18
	4	65.6	97.8	81.7	2.69	4.0	1.9	2.3	1.17
	6	79.6	> 99.9	89.8	3.18	4.4	2.0	2.4	1.19
	8	88.1	> 99.9	94.1	3.52	4.6	2.0	2.3	1.19
	24	98.2	> 99.9	99.1	3.93	4.9	1.7	2.2	1.28

^a Calculated via ¹H NMR spectroscopy. ^b Calculated *via* GPC against narrow molecular weight PEG calibrants.

Table S4. Percentage residuals from fitting of GPC chromatograms at various time points for the thermal polymerisations.

Temperature (°C)	Time (h)	Total monomer conversion (%) ^a	Residual (%) ^b		
			Fronting	Tailing	Total
100	0.25	4.3	0.0	0.0	0.0
	1	11.9	0.0	1.3	1.3
	2	16.6	0.1	2.5	2.6
	4	32.4	0.1	3.7	3.8
	6	40.3	0.2	4.8	5.0
	8	42.7	0.2	5.2	5.4
	10	46.5	0.3	6.2	6.5
	24	63.1	0.8	11.4	12.2
	48	72.3	1.2	11.9	13.1
	72	79.3	1.8	14.5	16.3
96	89.1	4.9	16.5	21.4	
110	0.25	4.6	0.0	0.0	0.0
	1	13.9	0.7	2.1	2.8
	2	26.0	0.8	2.2	3.0
	4	38.5	1.6	1.6	3.2
	6	46.8	1.7	1.4	3.1
	24	74.9	5.5	6.5	12.0
	48	91.4	9.4	11.1	20.5
	72	95.1	13.6	18.8	32.4
120	0.25	7.6	0.0	0.0	0.0
	1	22.9	2.1	0.9	3.0
	2	35.0	0.8	0.3	1.1
	4	49.8	0.7	0.5	1.2
	6	58.5	2.2	1.7	3.9
	24	83.6	8.4	9.1	17.5
48	95.0	14.6	14.1	28.7	

^a Calculated from ¹H NMR spectroscopy. ^b Determined from peak fitting of GPC chromatograms.

Table S5. Percentage residuals from fitting of GPC chromatograms at various time points for the Sn(Oct)₂ catalysed polymerisations.

Catalyst Loading (wt%)	Time (h)	Total monomer conversion (%) ^a	Residual (%) ^b		
			Fronting	Tailing	Total
0.1	0.25	8.2	0.0	0.0	0.0
	1	23.5	0.0	0.8	0.8
	2	33.3	0.0	1.6	1.6
	6	49.5	0.1	4.9	5.0
	8	51.6	0.3	7.4	7.7
	10	54.5	6.3	7.7	14.0
	24	73.1	11.0	16.1	27.1
0.2	0.25	6.0	0	0	0
	1	26.1	0.1	1.4	1.5
	2	34.5	1.3	1.8	3.1
	4	44.8	3.7	8.8	12.5
	6	54.2	3.8	10.9	14.7
	8	58.5	3.6	12.0	15.6
	10	60.9	4.4	11.0	15.4
24	78.1	2.9	13.4	16.3	
0.4	0.25	5.3	0.0	0.0	0.0
	1	24.9	0.3	0.0	0.3
	2	36.5	0.0	0.3	0.3
	4	47.1	6.6	0.4	7.0
	6	55.9	5.9	1.6	7.5
	8	59.4	4.3	7.5	11.8
	10	62.4	7.1	17.0	24.1
24	80.1	3.8	17.4	21.2	

^a Calculated from ¹H NMR spectroscopy. ^b Determined from peak fitting of GPC chromatograms.

Table S6. Percentage residuals from fitting of GPC chromatograms at various time points for the Sn(OTf)₂ catalysed polymerisations.

Catalyst Loading (wt%)	Time (h)	Total monomer conversion (%) ^a	Residual (%) ^b		
			Fronting	Tailing	Total
0.1	0.25	4.3	2.5	2.5	5.0
	1	15.3	2.9	4.9	7.8
	2	19.9	3.1	8.6	11.7
	4	32.9	6.1	16.6	22.7
	6	42.1	4.3	20.6	24.9
	8	48.6	5.5	24.2	29.7
	24	76.8	10.3	29.1	39.4
0.4	0.25	9.1	5.9	4.0	9.9
	1	49.8	11.7	31.7	43.4
	2	65.7	13.3	34.4	47.7
	4	81.7	20.8	31.5	52.3
	6	89.7	22.6	29.7	52.3
	8	94.0	25.5	26.9	52.4
	24	99.0	28.9	29.3	58.2

^a Calculated from ¹H NMR spectroscopy. ^b Determined from peak fitting of GPC chromatograms.

Supporting Figures

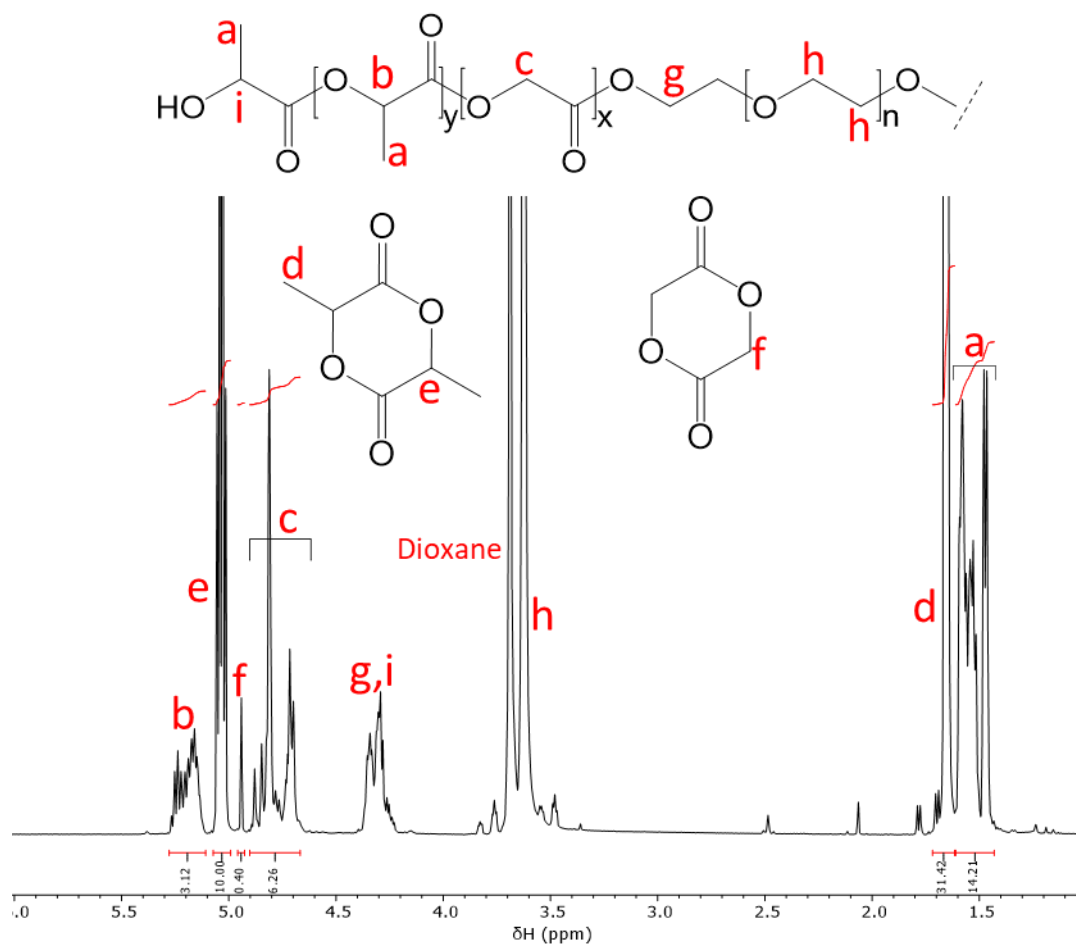


Figure S1. ^1H NMR spectrum (500 MHz, 25 °C, CDCl_3) of the thermal polymerisation at 100 °C after 24 h, along with resonance assignment and integration to show calculation of the monomer conversion.

Calculation of monomer conversion:

$$\text{L \% conversion} = \text{integration of a} / \text{integration a} + \text{d} = 14.21 / (14.21 + 31.42) \times 100\% = 31.1\%$$

$$\text{G \% conversion} = \text{integration of c} / \text{integration c} + \text{f} = 6.26 / (6.26 + 0.40) \times 100\% = 94.0\%$$

Calculation of repeat units (RUs)

$$\text{RU}_L = (\text{conversion of L} \times \text{initial moles of L}) / \text{moles of PEG} = (31.1\% \times 13.3) / 0.667 = 12.4$$

$$\text{RU}_G = (\text{conversion of G} \times \text{initial moles of G}) / \text{moles of PEG} = (94.0\% \times 3.33) / 0.667 = 4.7$$

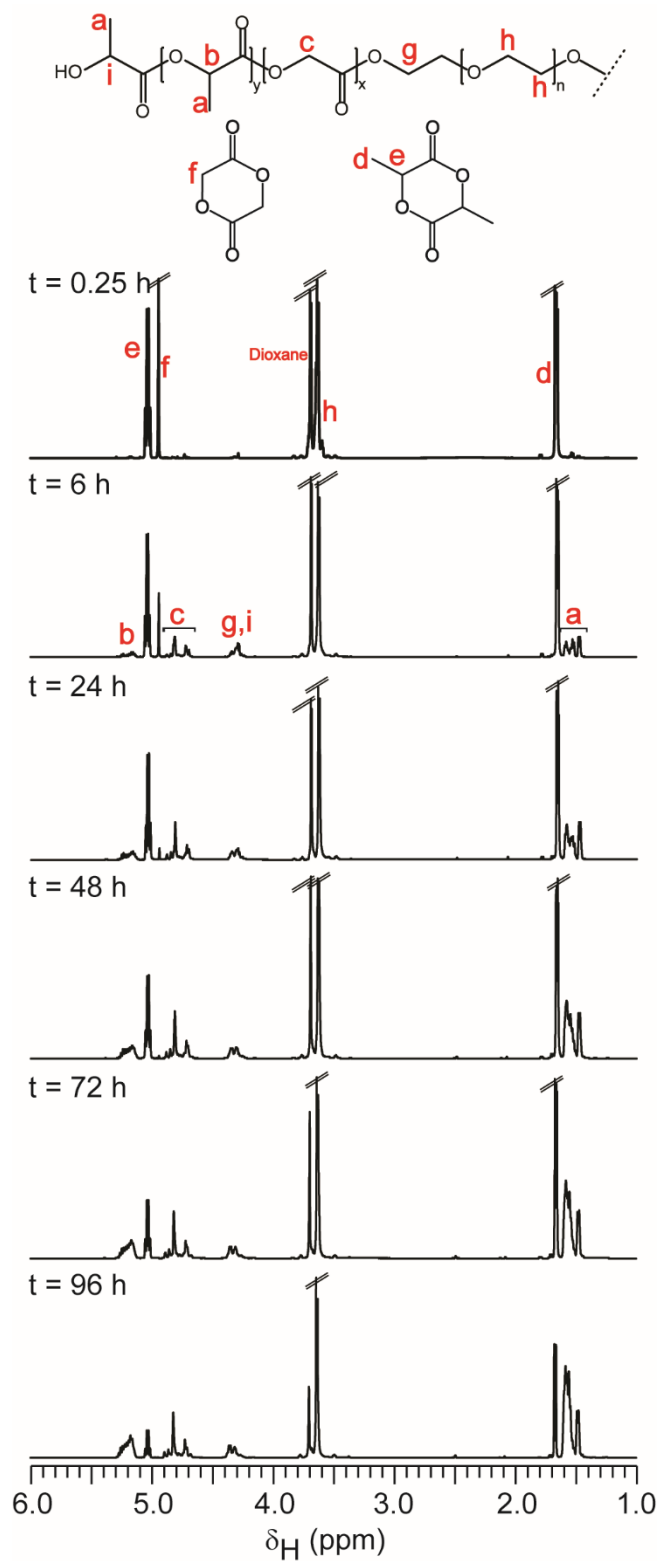


Figure S2. Selected ^1H NMR spectra (500 MHz, 25°C , CDCl_3) following thermal polymerisation at 100°C .

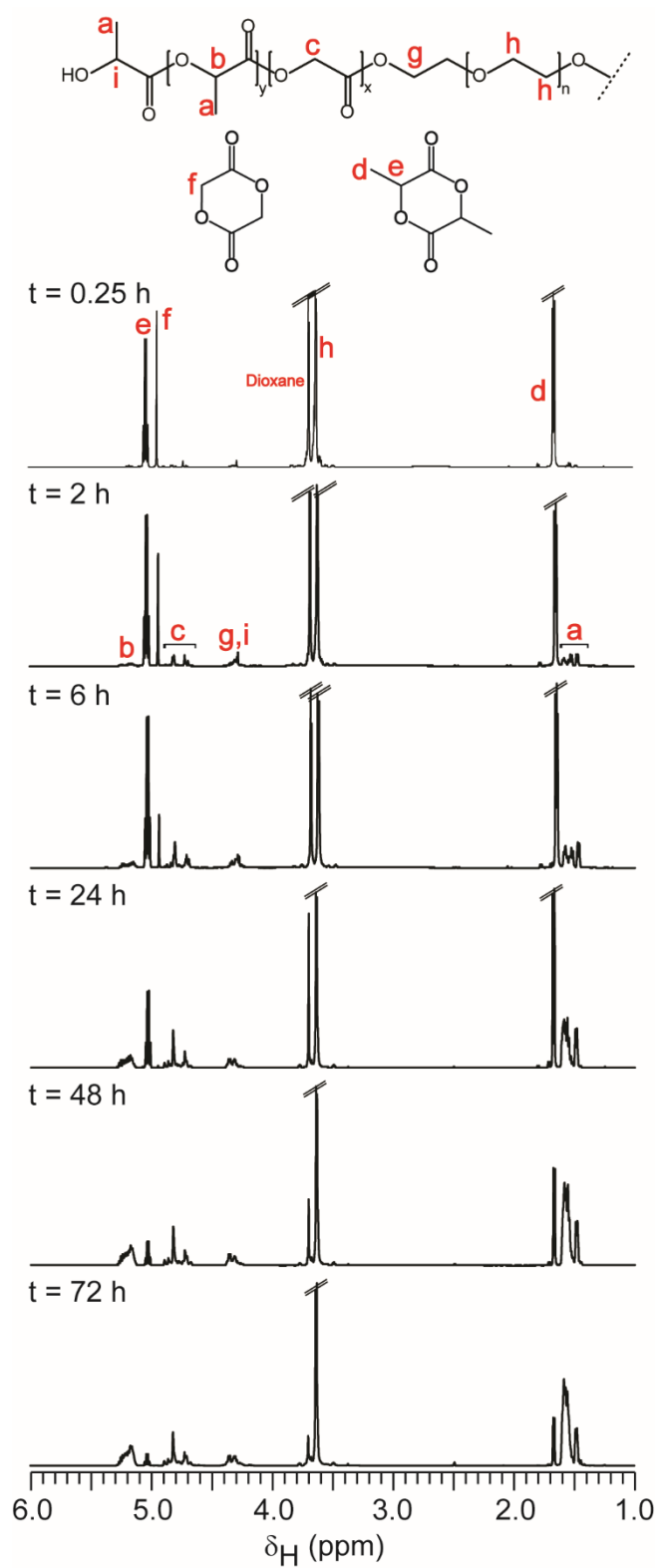


Figure S3. Selected ^1H NMR spectra (500 MHz, 25 °C, CDCl_3) following thermal polymerisation at 110 °C.

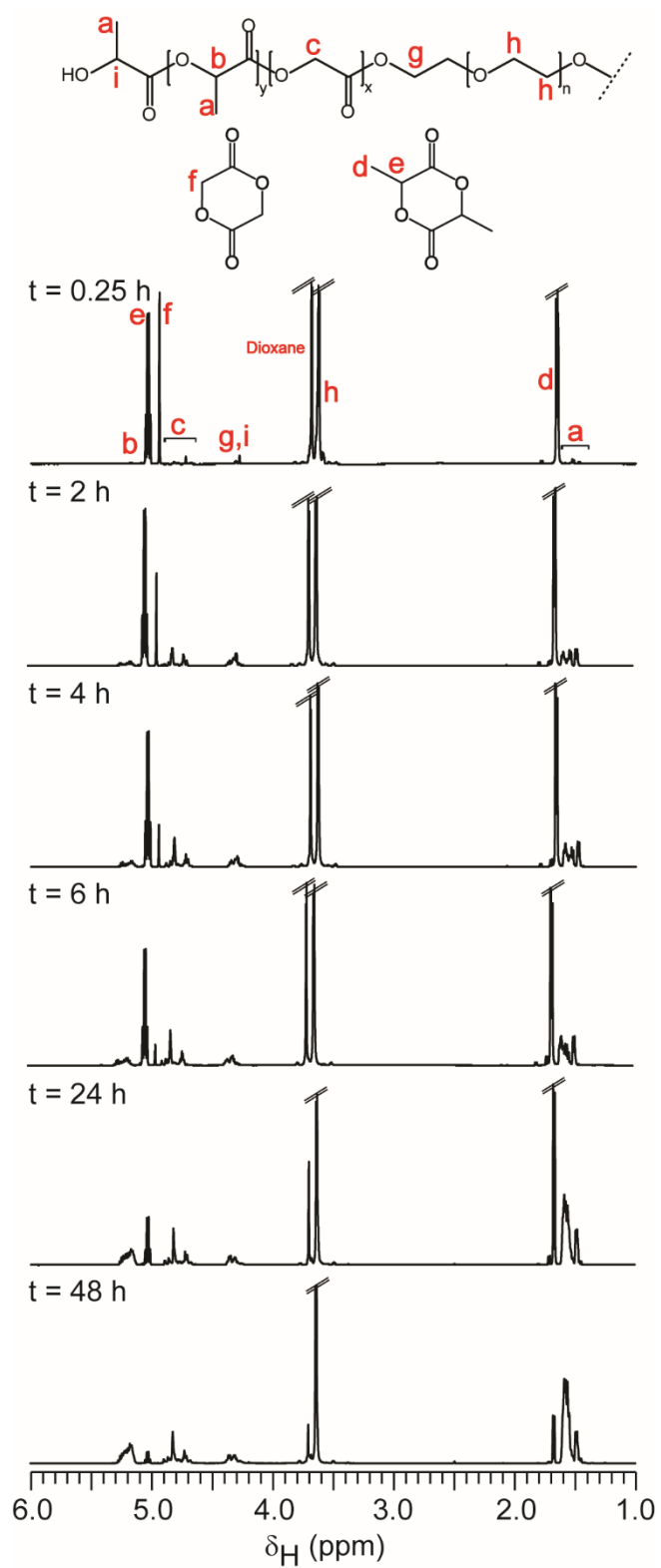


Figure S4. Selected ^1H NMR spectra (500 MHz, $25\text{ }^\circ\text{C}$, CDCl_3) following thermal polymerisation at $120\text{ }^\circ\text{C}$.

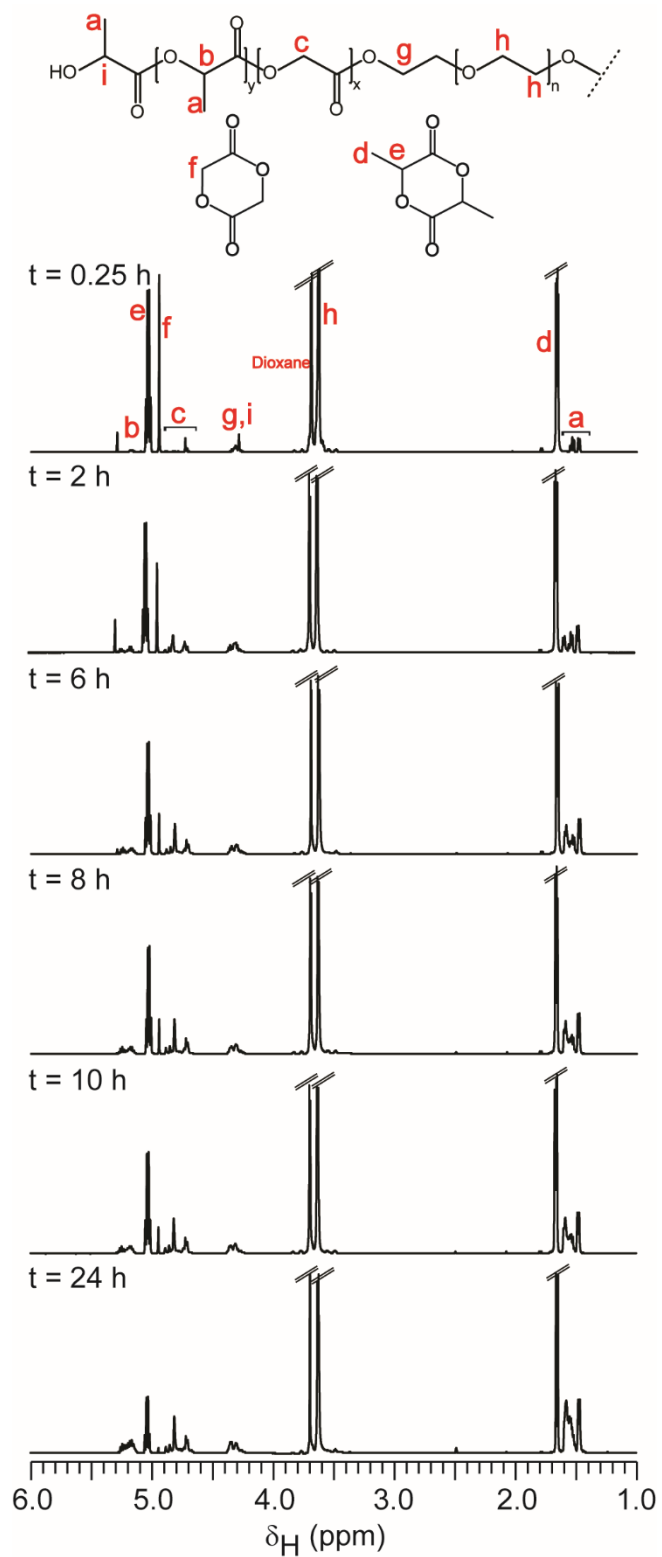


Figure S5. Selected ^1H NMR spectra (500 MHz, 25 $^\circ\text{C}$, CDCl_3) following $\text{Sn}(\text{Oct})_2$ (0.1 wt%) catalysed polymerisation at 100 $^\circ\text{C}$.

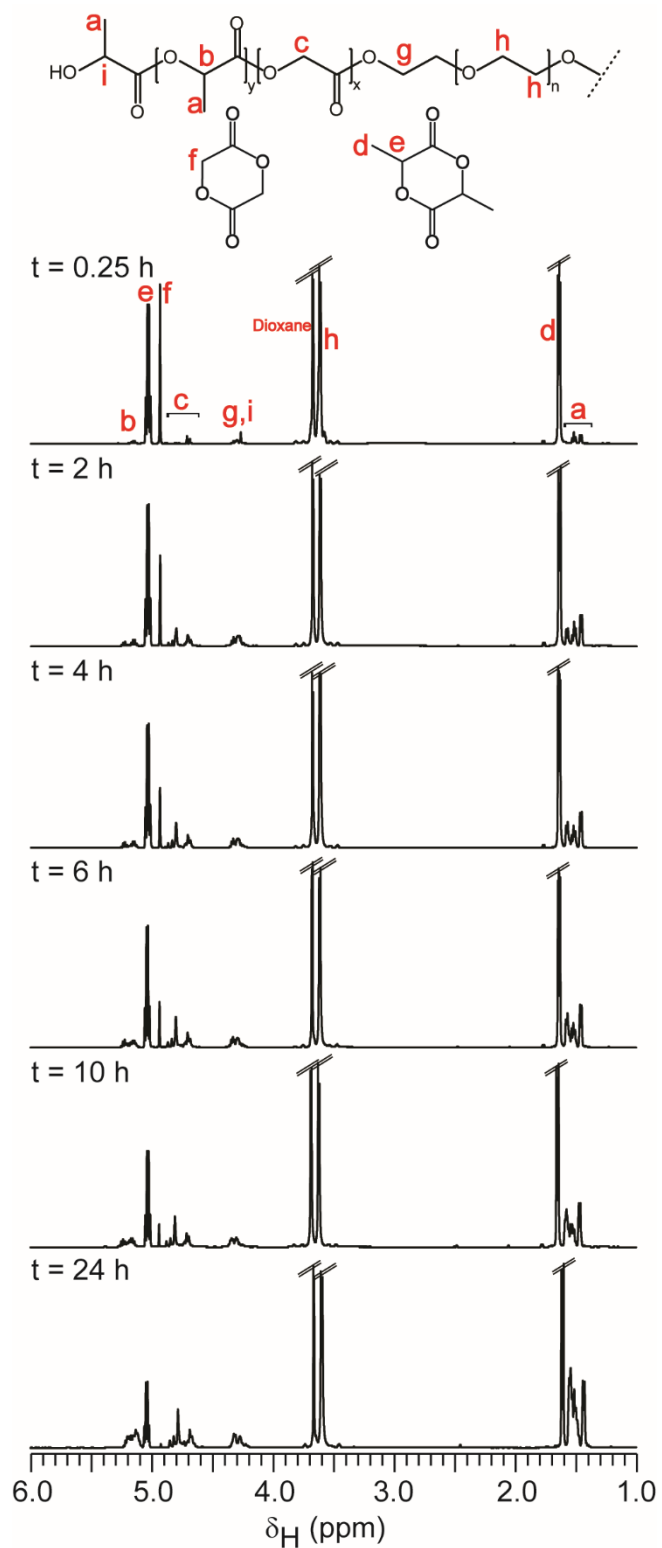


Figure S6. Selected ^1H NMR spectra (500 MHz, 25 °C, CDCl_3) following $\text{Sn}(\text{Oct})_2$ (0.2 wt%) catalysed polymerisation at 100 °C.

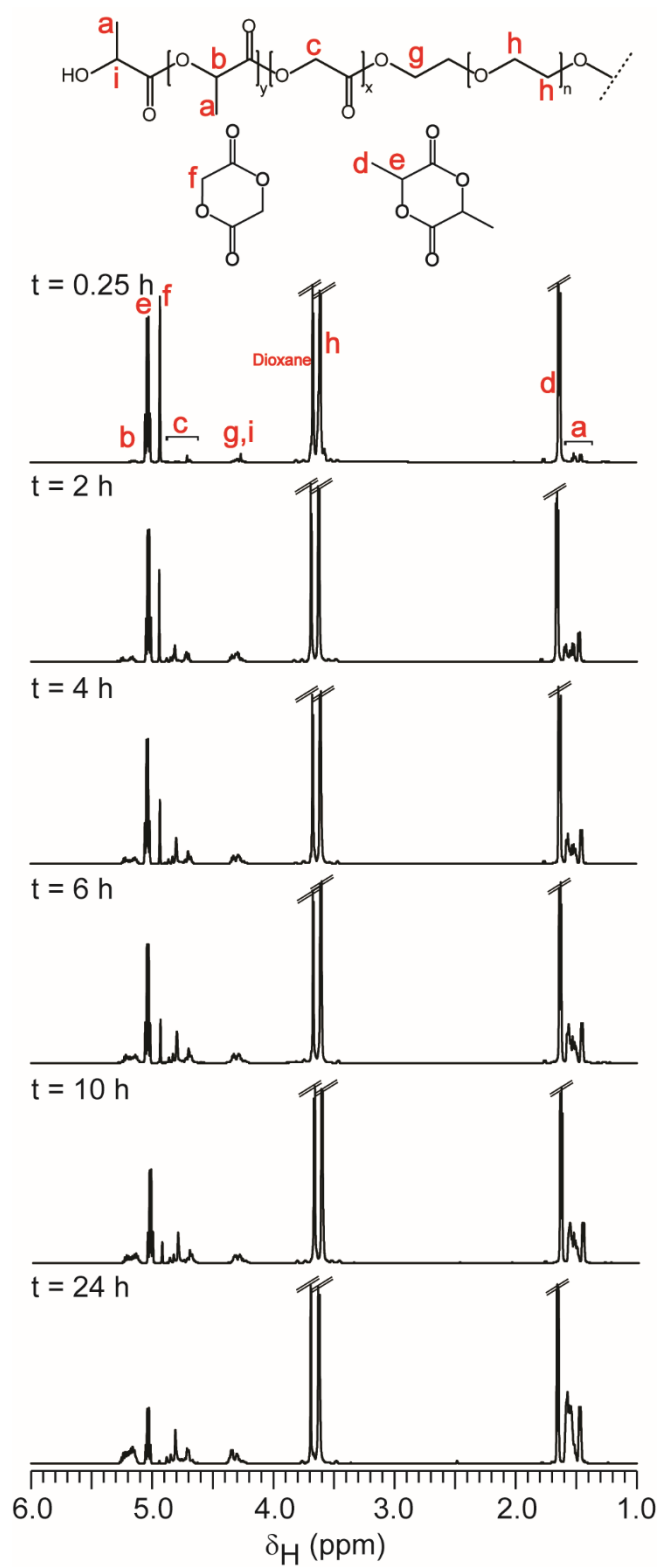


Figure S7. Selected ^1H NMR spectra (500 MHz, 25 °C, CDCl_3) following $\text{Sn}(\text{Oct})_2$ (0.4 wt%) catalyzed polymerisation at 100 °C.

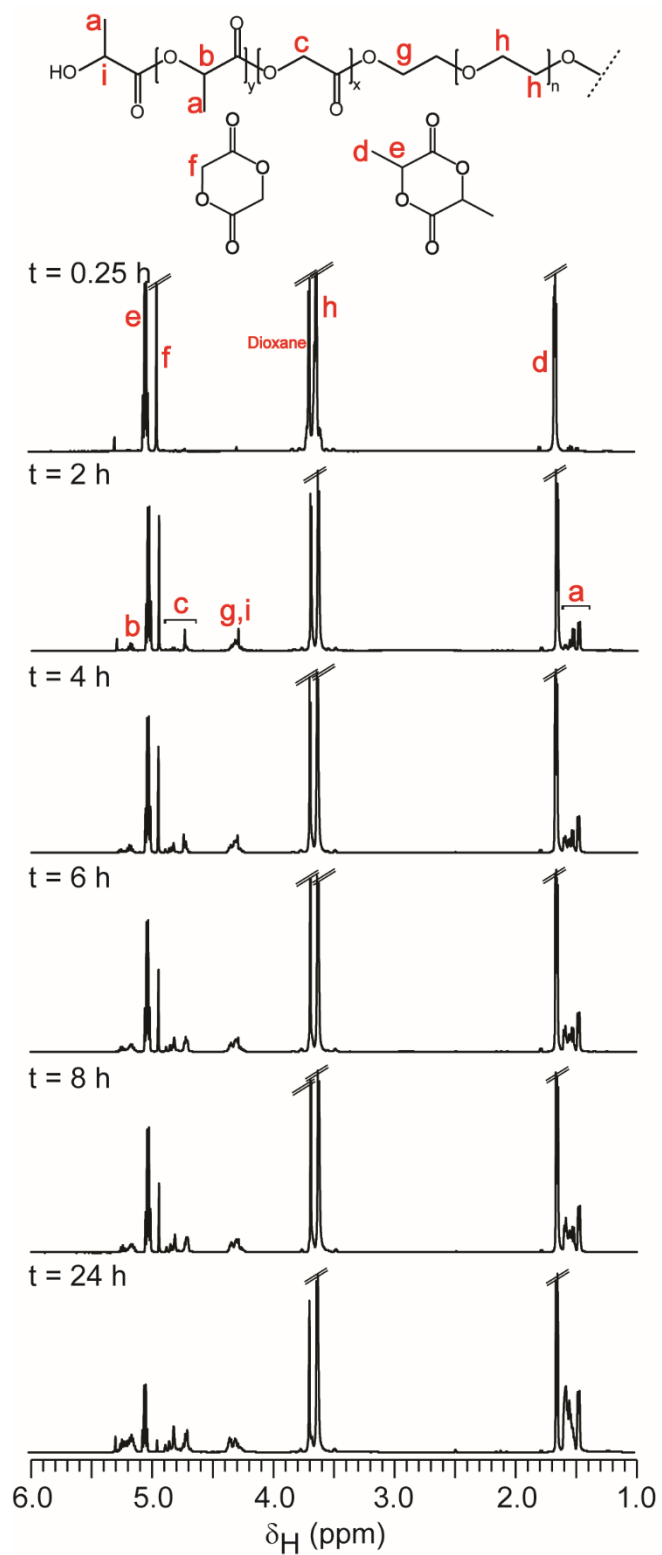


Figure S8. Selected ^1H NMR spectra (500 MHz, 25 $^{\circ}\text{C}$, CDCl_3) following $\text{Sn}(\text{OTf})_2$ (0.1 wt%) catalysed polymerisation at 100 $^{\circ}\text{C}$.

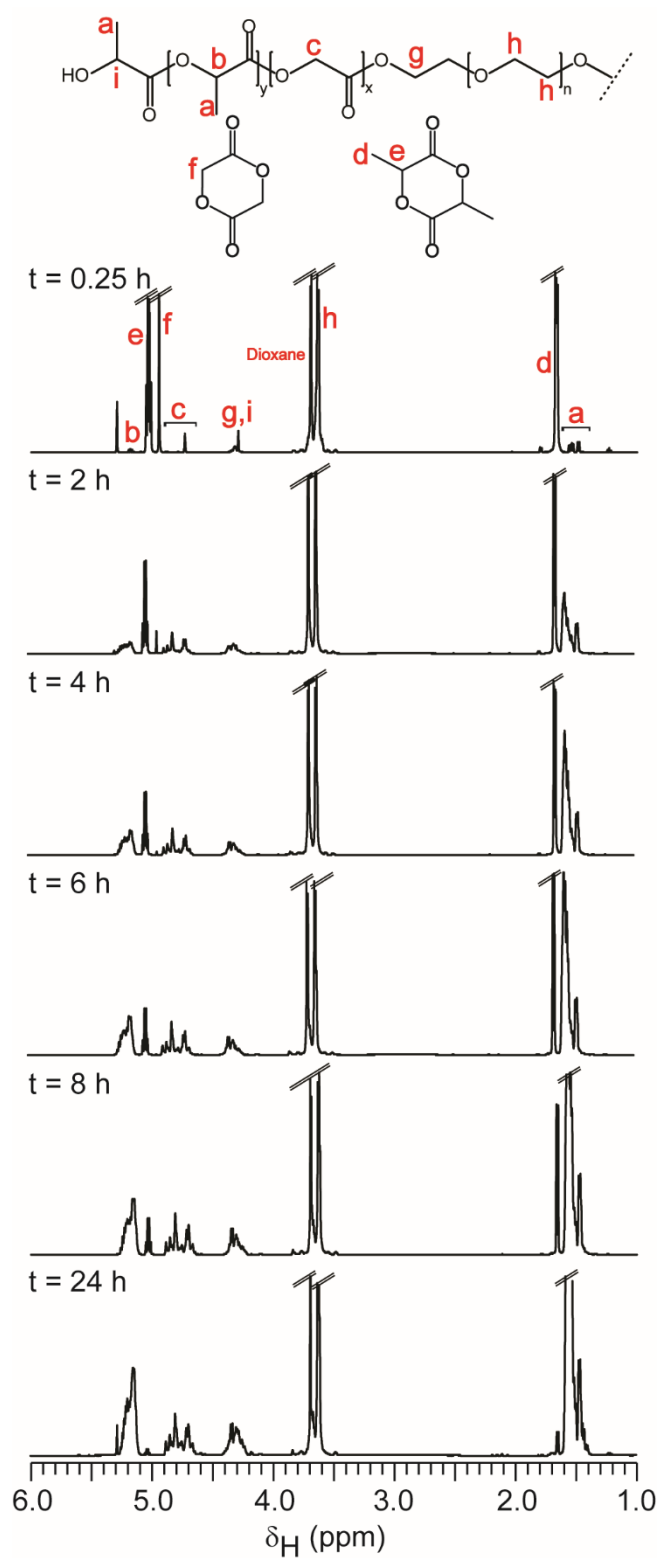


Figure S9. Selected ^1H NMR spectra (500 MHz, 25 $^\circ\text{C}$, CDCl_3) following $\text{Sn}(\text{OTf})_2$ (0.4 wt%) catalysed polymerisation at 100 $^\circ\text{C}$.

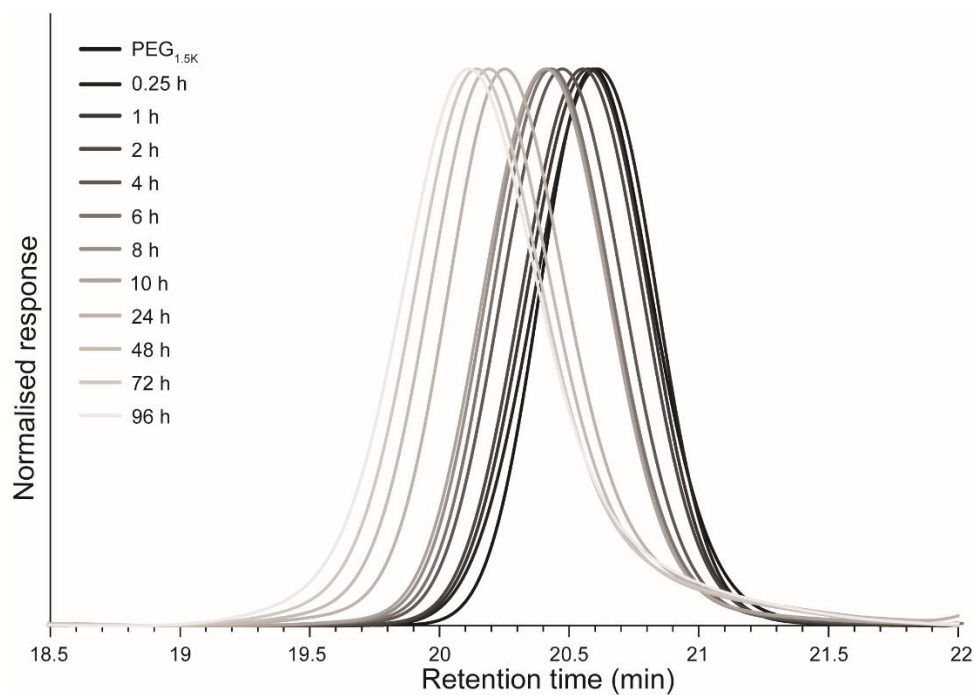


Figure S10. GPC differential refractive index (DRI) chromatograms showing molecular weight distribution as a function of time for the thermal polymerisation at 100 °C.

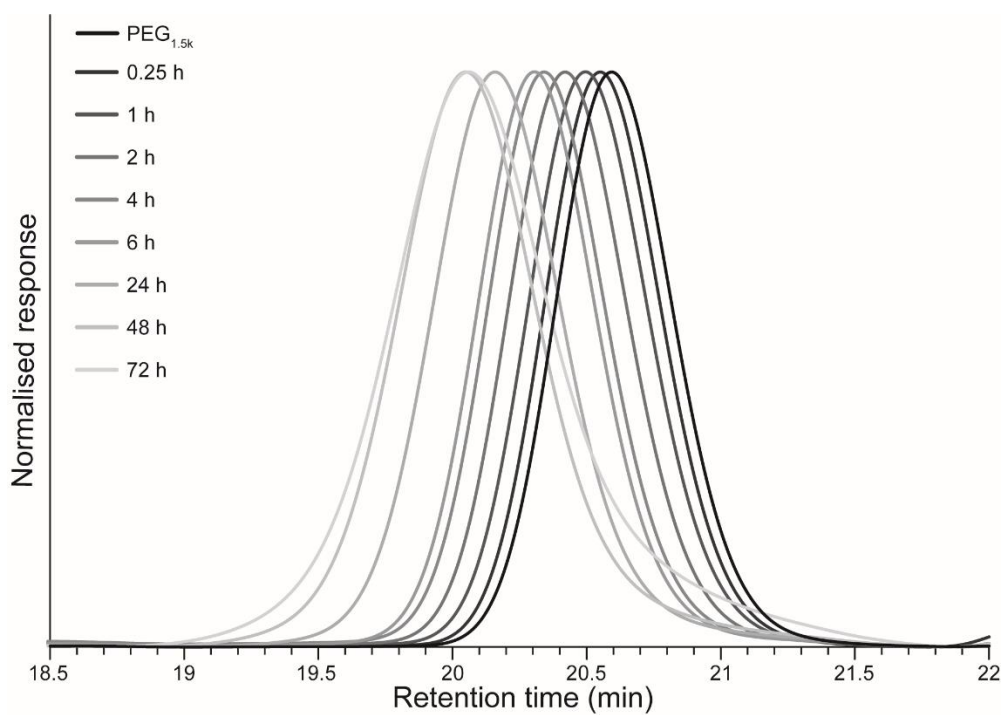


Figure S11. GPC DRI chromatograms showing molecular weight distribution as a function of time for the thermal polymerisation at 110 °C.

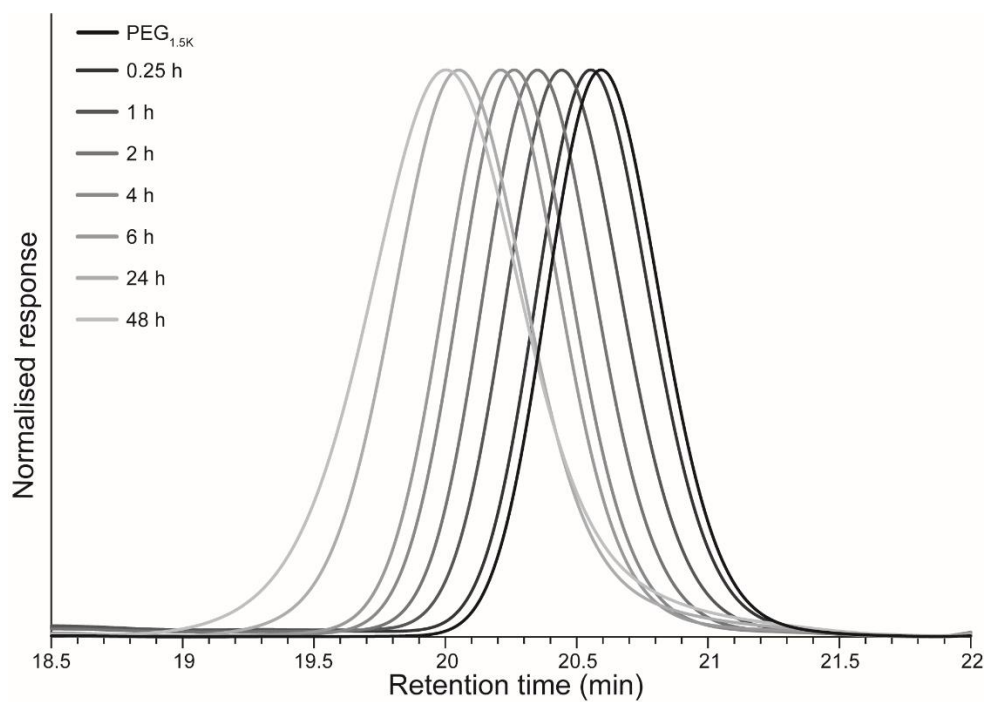


Figure S12. GPC DRI chromatograms showing molecular weight distribution as a function of time for the thermal polymerisation at 120 °C.

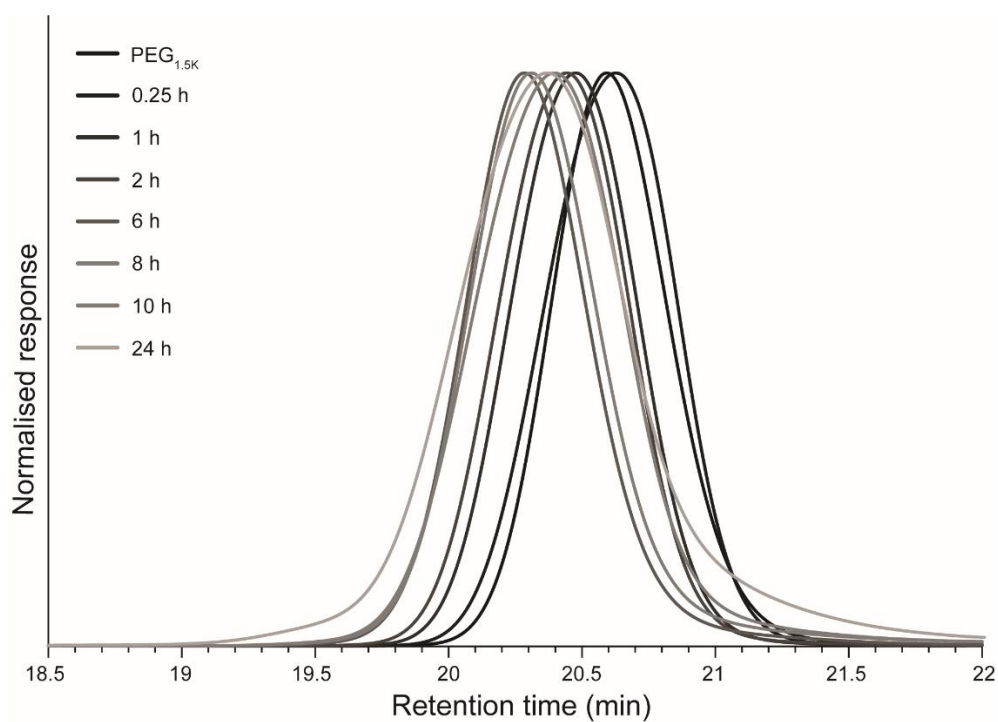


Figure S13. GPC DRI chromatograms showing molecular weight distribution as a function of time for the Sn(Oct)₂ (0.1 wt%) catalysed polymerisation at 100 °C.

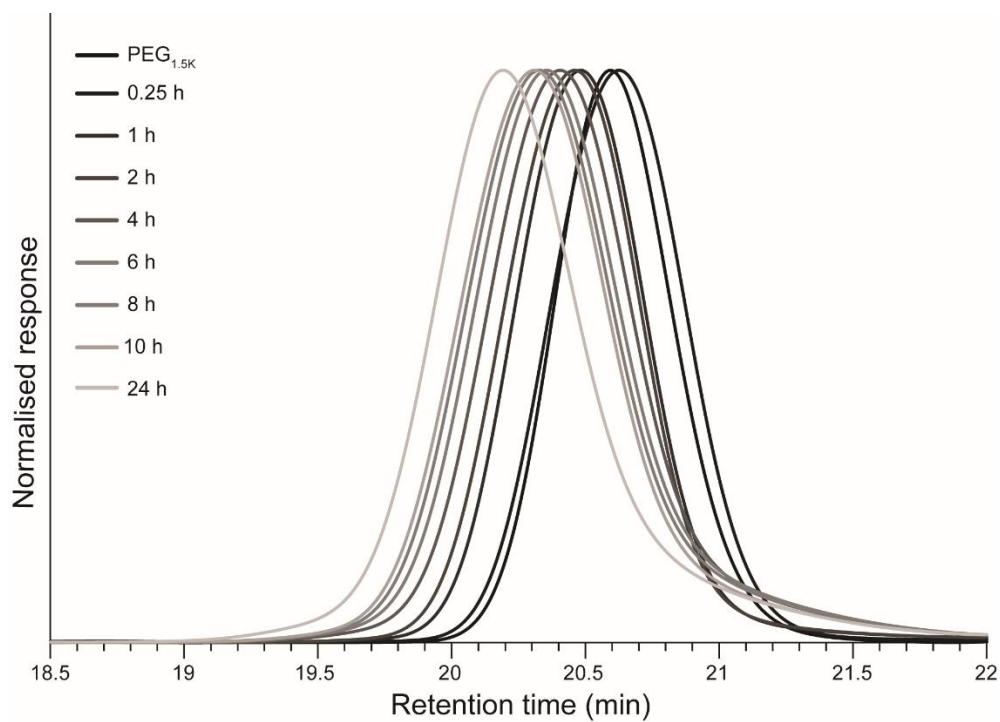


Figure S14. GPC DRI chromatograms showing molecular weight distribution as a function of time for the Sn(Oct)₂ (0.2 wt%) catalysed polymerisation at 100 °C.

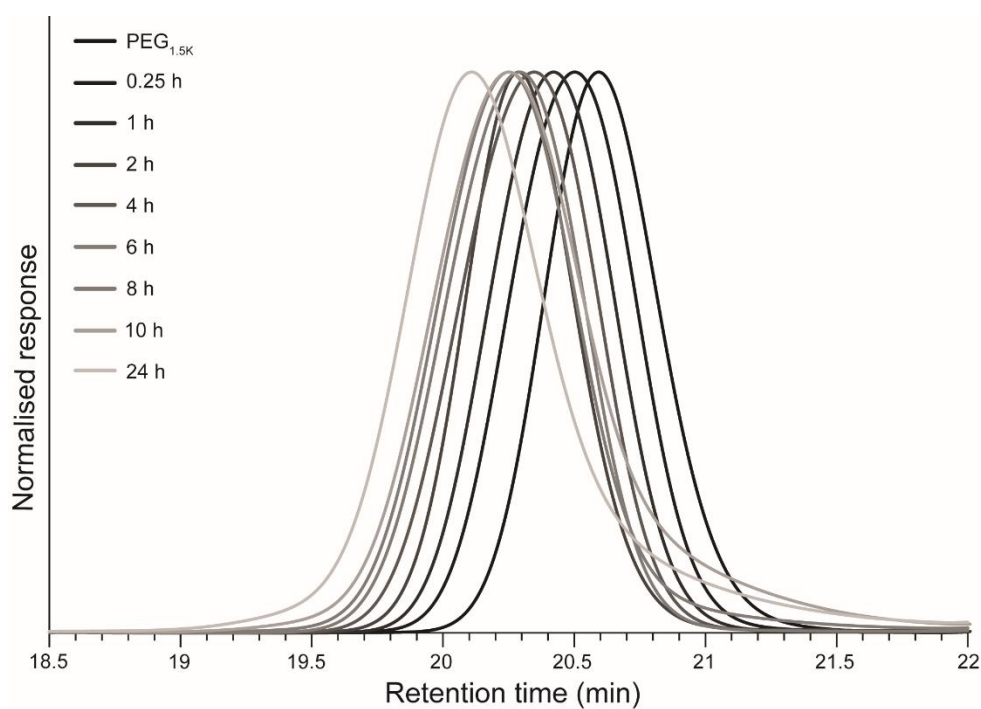


Figure S15. GPC DRI chromatograms showing molecular weight distribution as a function of time for the Sn(Oct)₂ (0.4 wt%) catalysed polymerisation at 100 °C.

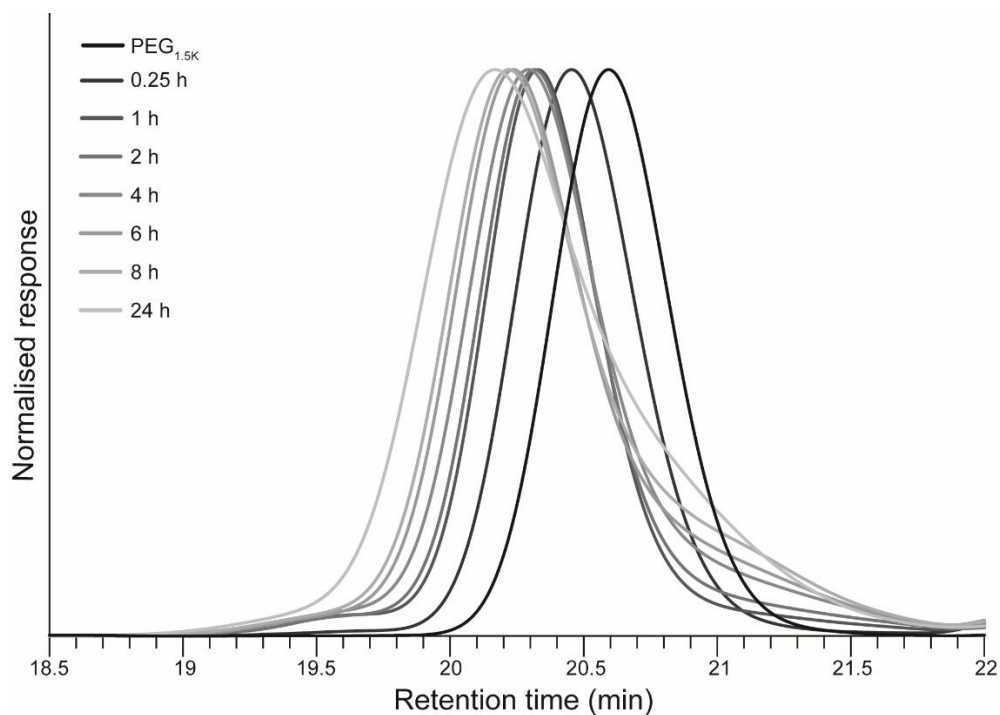


Figure S16. GPC DRI chromatograms showing molecular weight distribution as a function of time for the Sn(OTf)₂ (0.1 wt%) catalysed polymerisation at 100 °C.

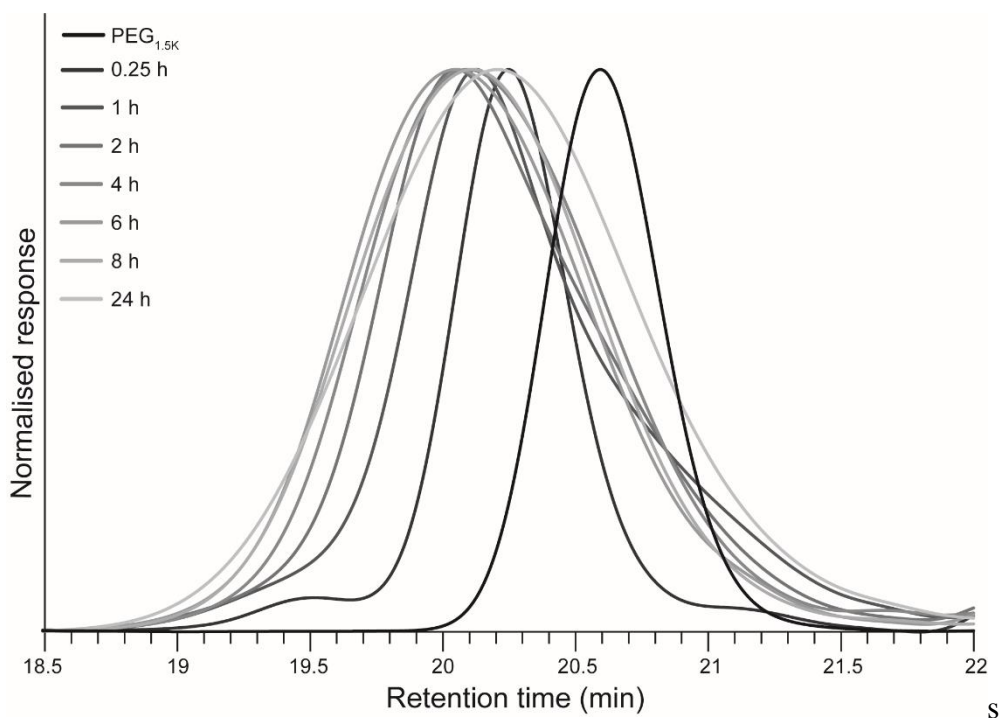


Figure S17. GPC DRI chromatograms showing molecular weight distribution as a function of time for the Sn(OTf)₂ (0.4 wt%) catalysed polymerisation at 100 °C.

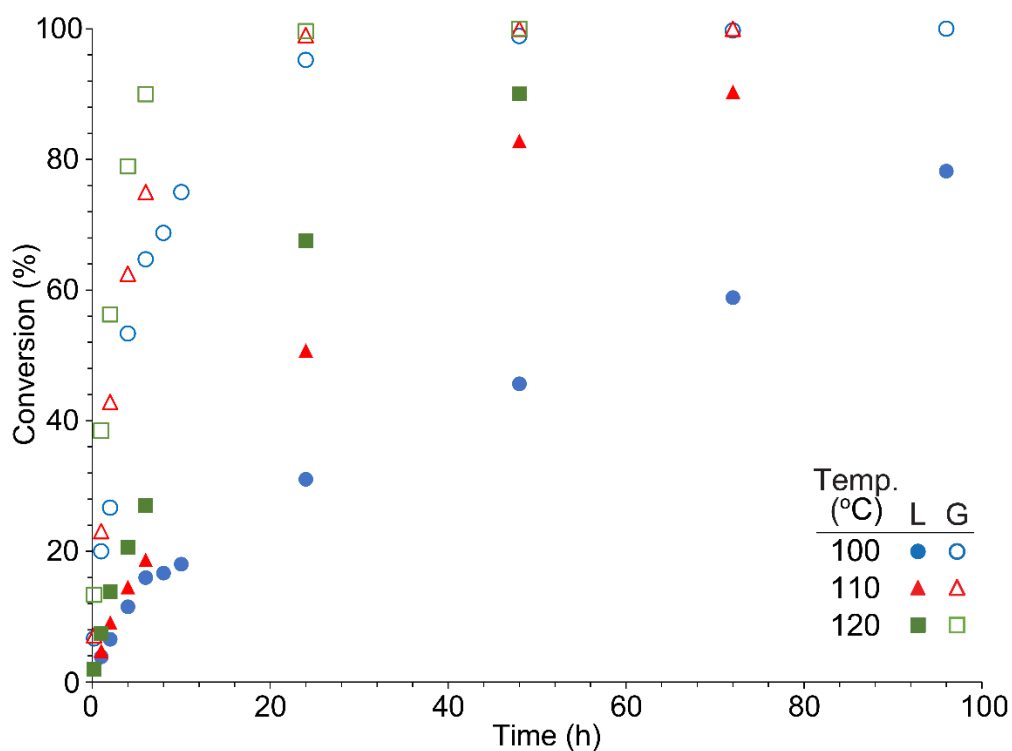


Figure S18. Lactide (L) and glycolide (G) conversion (%) *versus* time for thermal polymerisations conducted at 100, 110 and 120 °C.

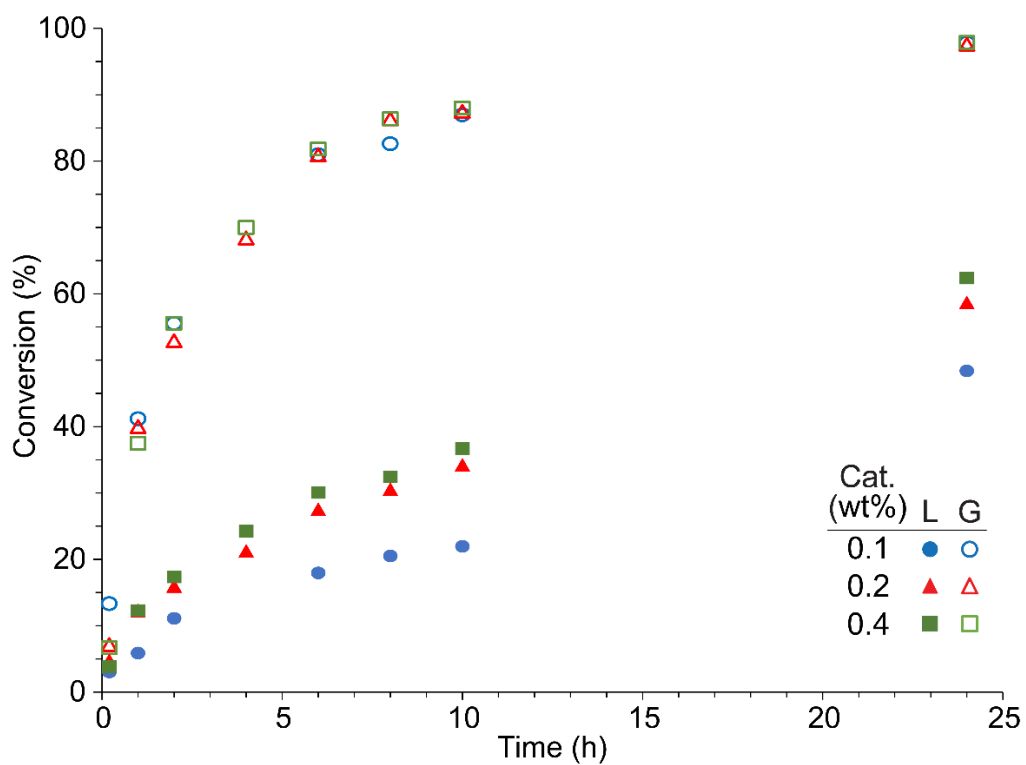


Figure S19. Lactide (L) and glycolide (G) conversion (%) *versus* time for Sn(Oct)₂ catalysed polymerisations conducted at catalyst loadings of 0.1, 0.2 and 0.4 wt%.

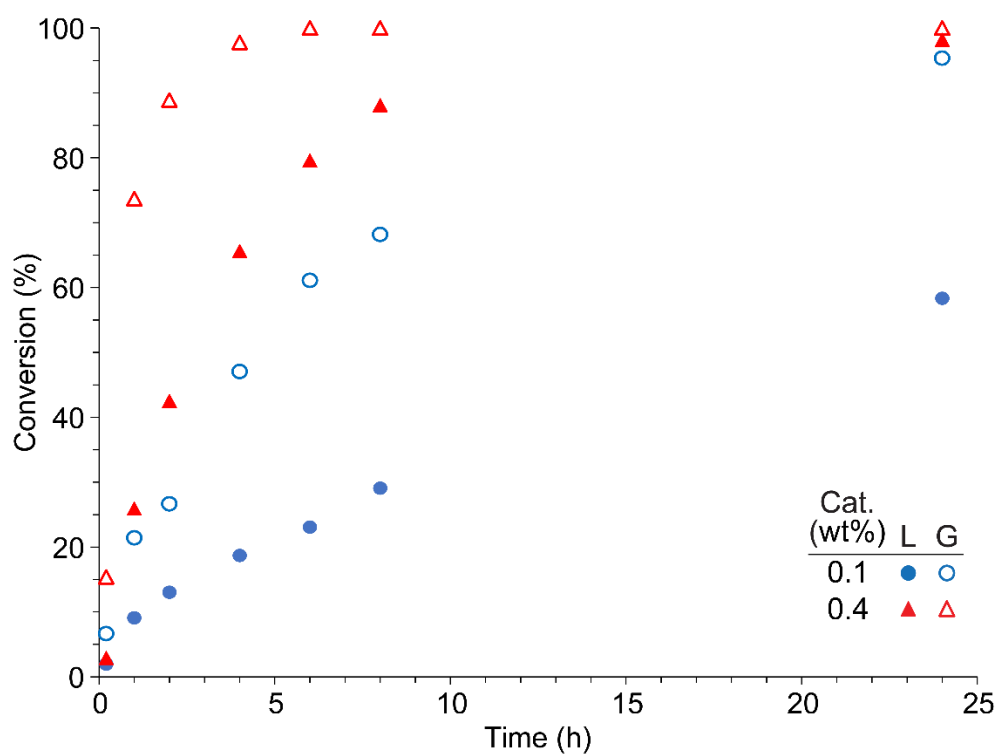


Figure S20. Lactide (L) and glycolide (G) conversion (%) *versus* time for Sn(OTf)₂ catalysed polymerisations conducted at catalyst loadings of 0.1 and 0.4 wt%.

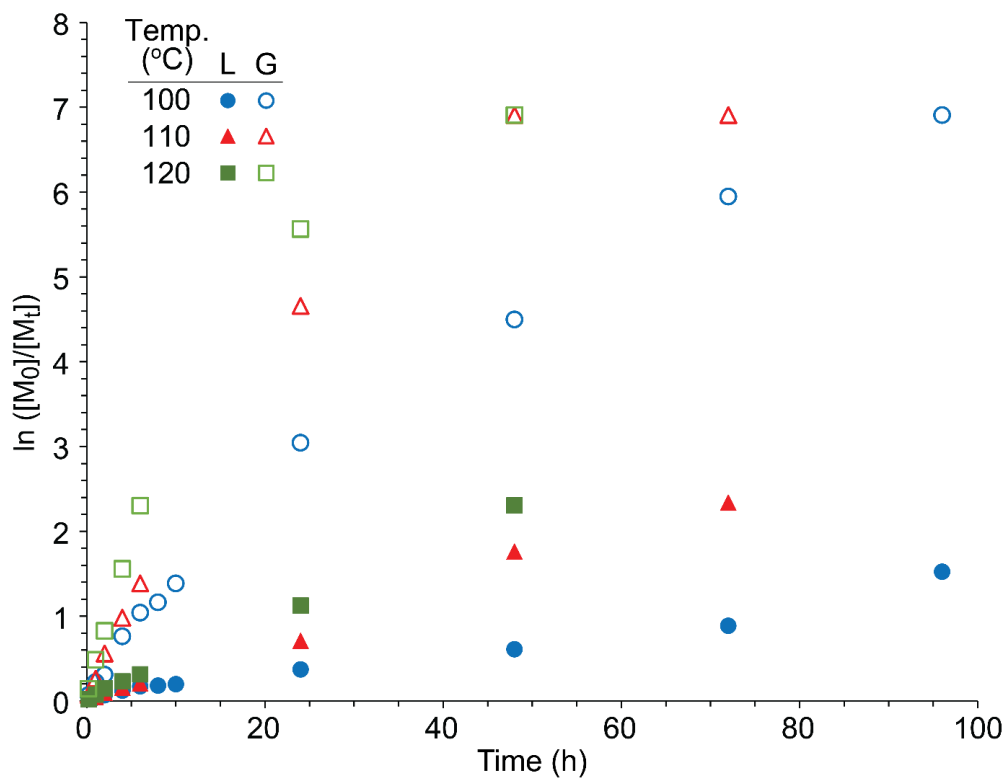


Figure S21. Pseudo-first-order $\ln([M]_0/[M]_t)$ versus time kinetic plots for thermal polymerisations conducted at 100, 110 and 120 °C.

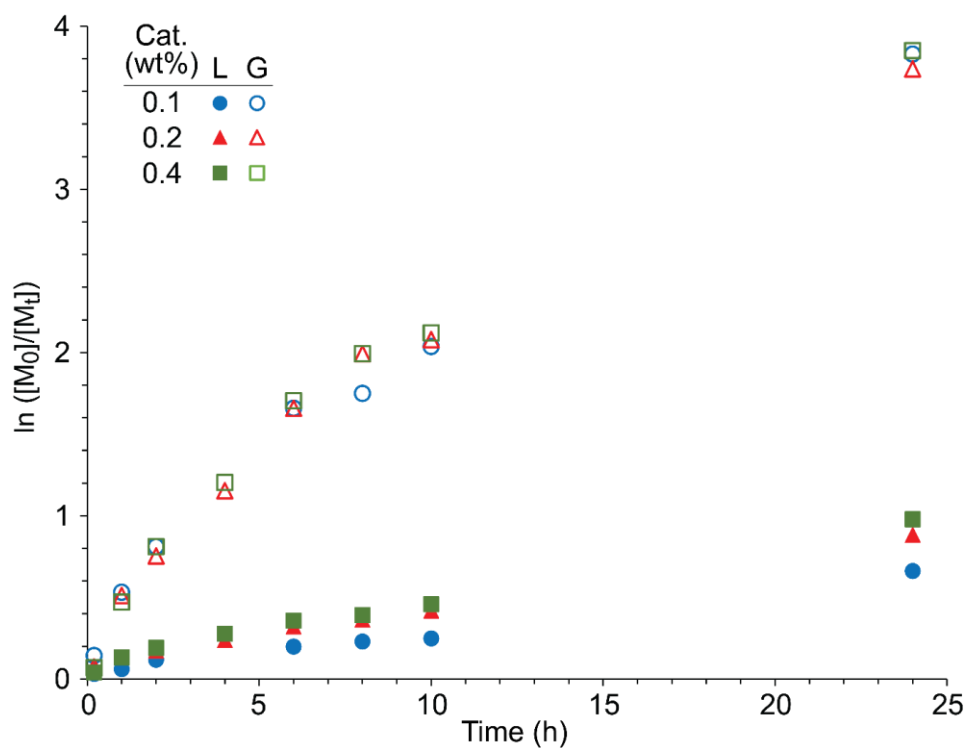


Figure S22. Pseudo-first-order $\ln([M]_0/[M]_t)$ versus time kinetic plots for $\text{Sn}(\text{Oct})_2$ catalysed polymerisations conducted at catalyst loadings of 0.1, 0.2 and 0.4 wt%.

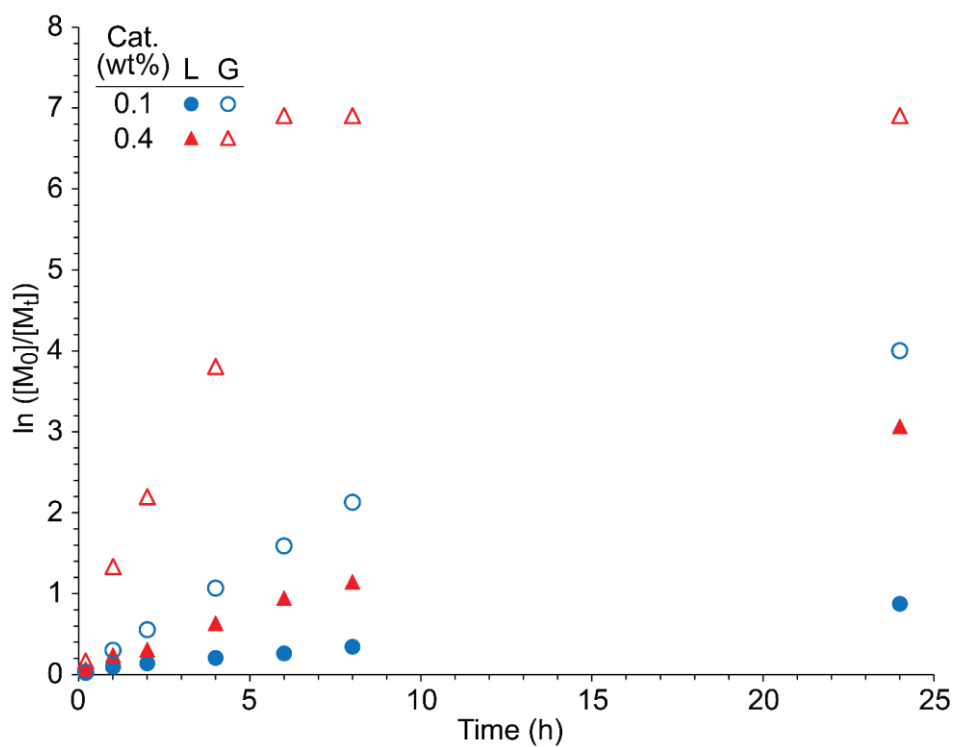


Figure S23. Pseudo-first-order $\ln([M]_0/[M]_t)$ versus time kinetic plots for Sn(OTf)₂ catalysed polymerisations conducted at catalyst loadings of 0.1 and 0.4 wt%.

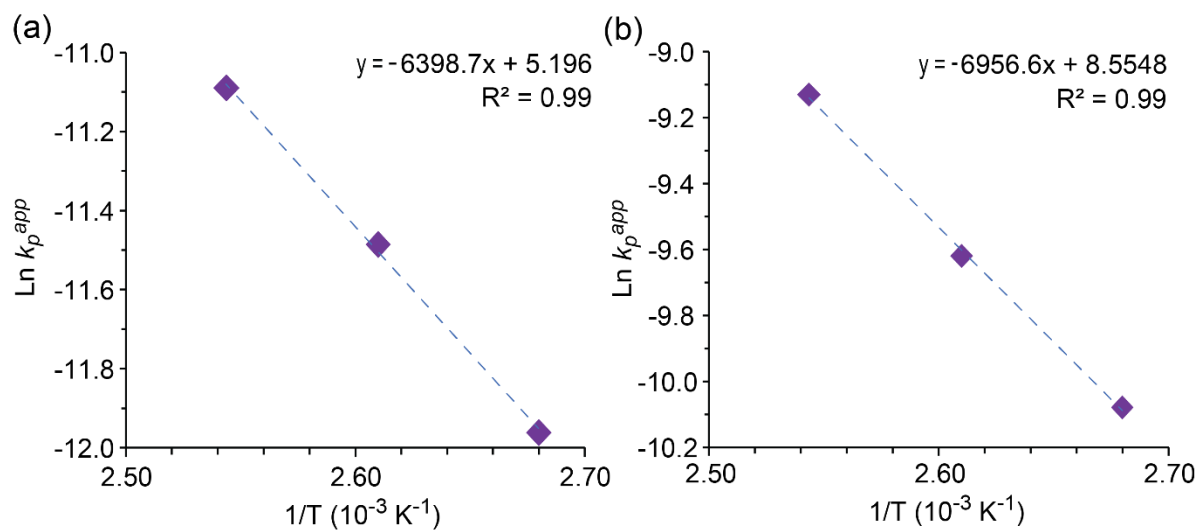


Figure S24. Arrhenius plots for thermal copolymerisation of (a) lactide and (b) glycolide.

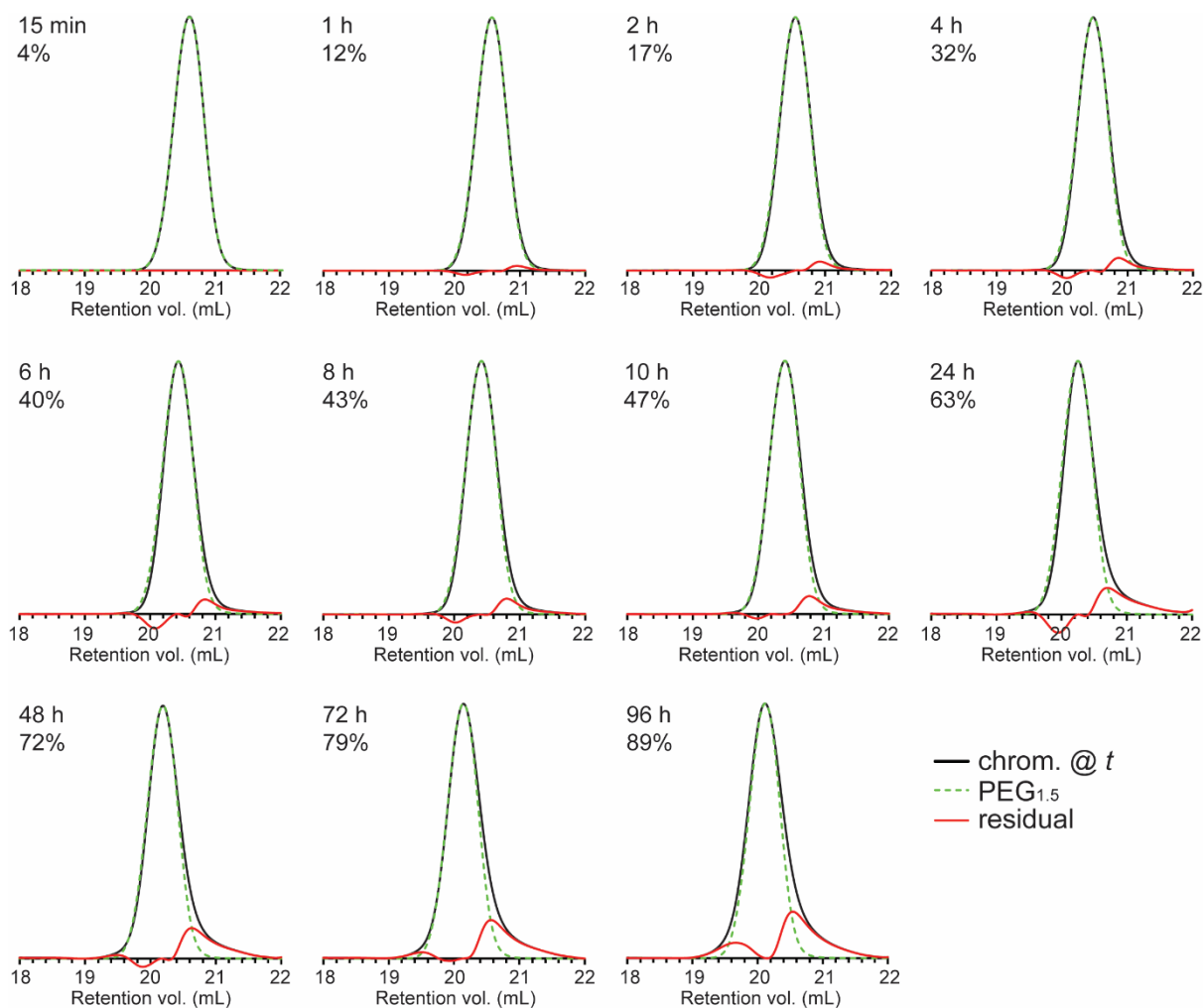


Figure S25. GPC DRI chromatograms over time for thermal polymerisation at 100 °C (solid black line) as compared to the initial peak shape (dashed grey line) and the resulting residual determination (solid red line). Total percentage monomer conversion at each time point is specified under the time.

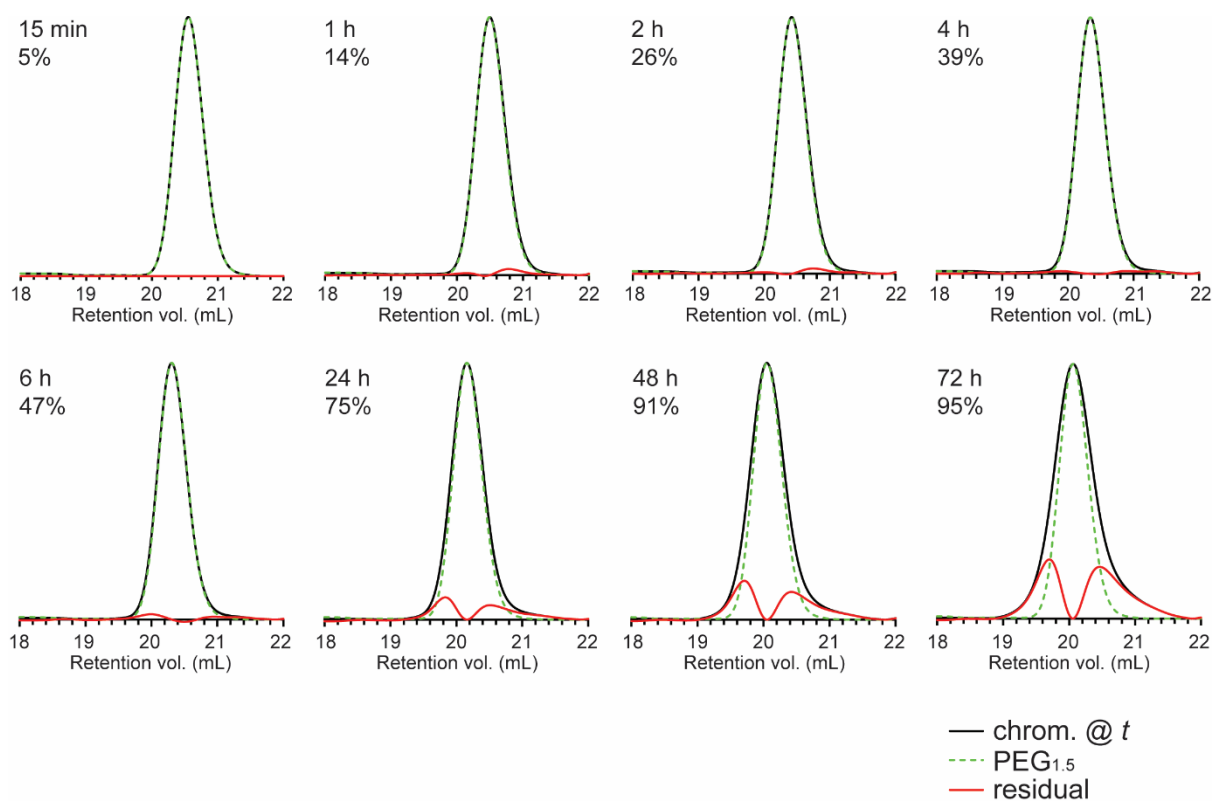


Figure S26. GPC DRI chromatograms over time for thermal polymerisation at 110 °C (solid black line) as compared to the initial peak shape (dashed grey line) and the resulting residual determination (solid red line). Total percentage monomer conversion at each time point is specified under the time.

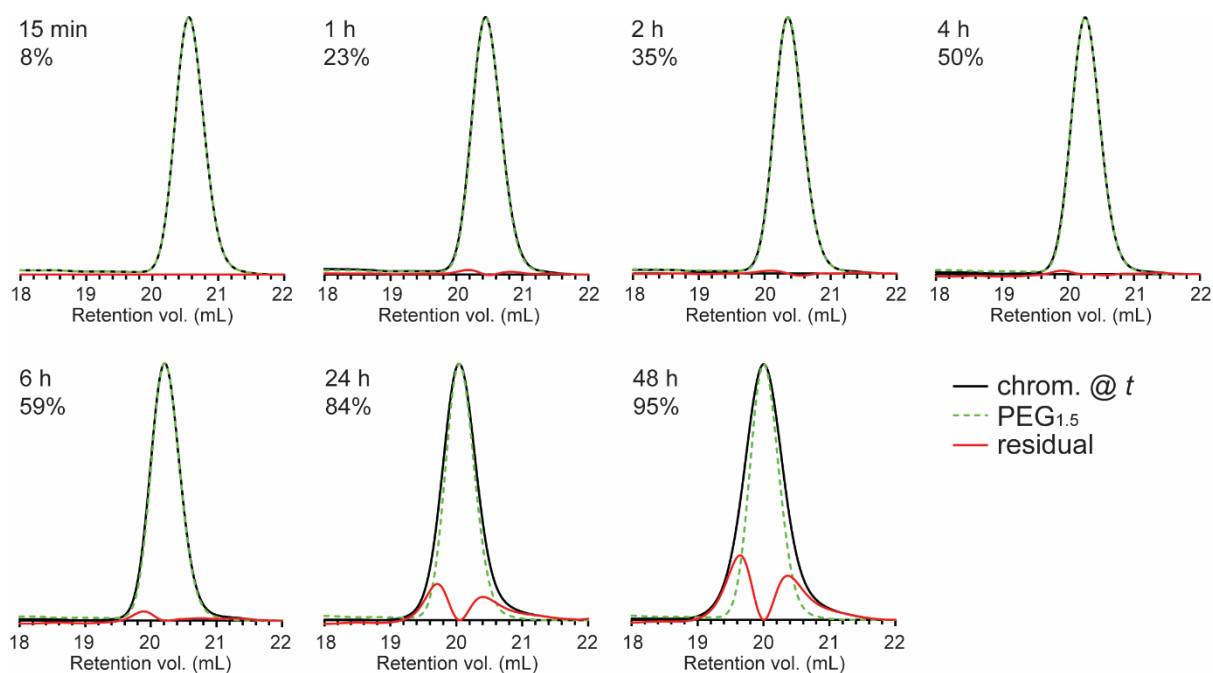


Figure S27. GPC DRI chromatograms over time for thermal polymerisation at 120 °C (solid black line) as compared to the initial peak shape (dashed grey line) and the resulting residual determination (solid red line). Total percentage monomer conversion at each time point is specified under the time.

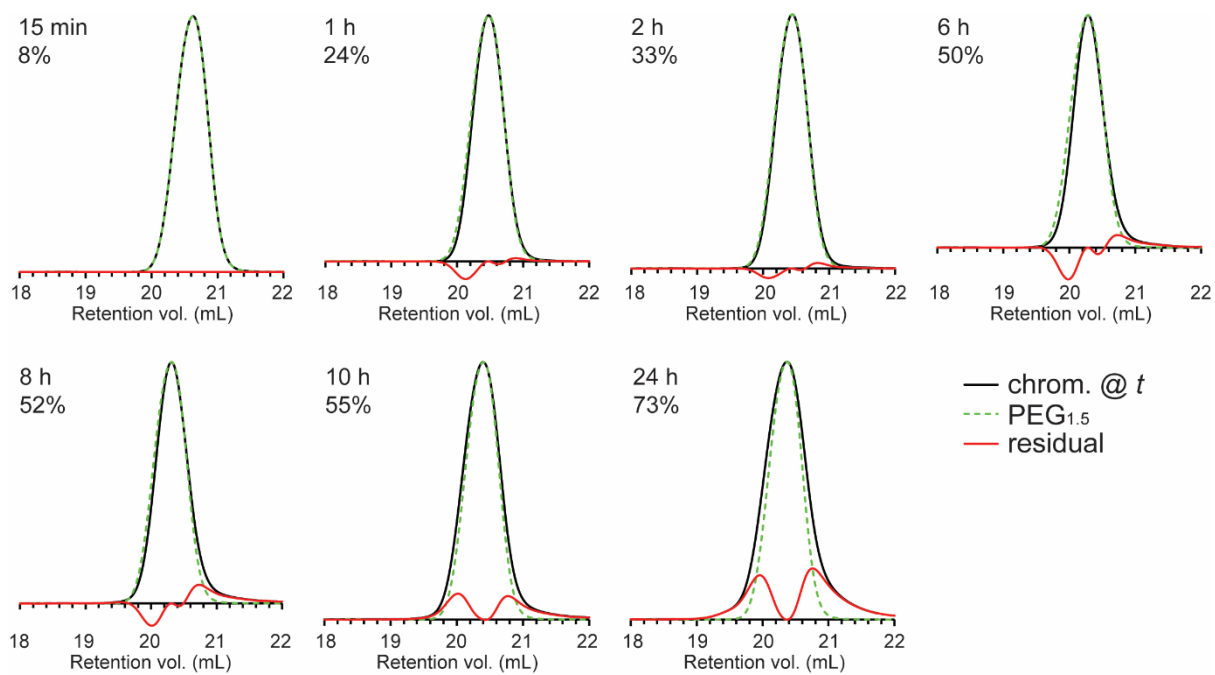


Figure S28. GPC DRI chromatograms over time for catalysed polymerisation with 0.1 wt% Sn(Oct)₂ at 100 °C (solid black line) as compared to the initial peak shape (dashed grey line) and the resulting residual determination (solid red line). Total percentage monomer conversion at each time point is specified under the time.

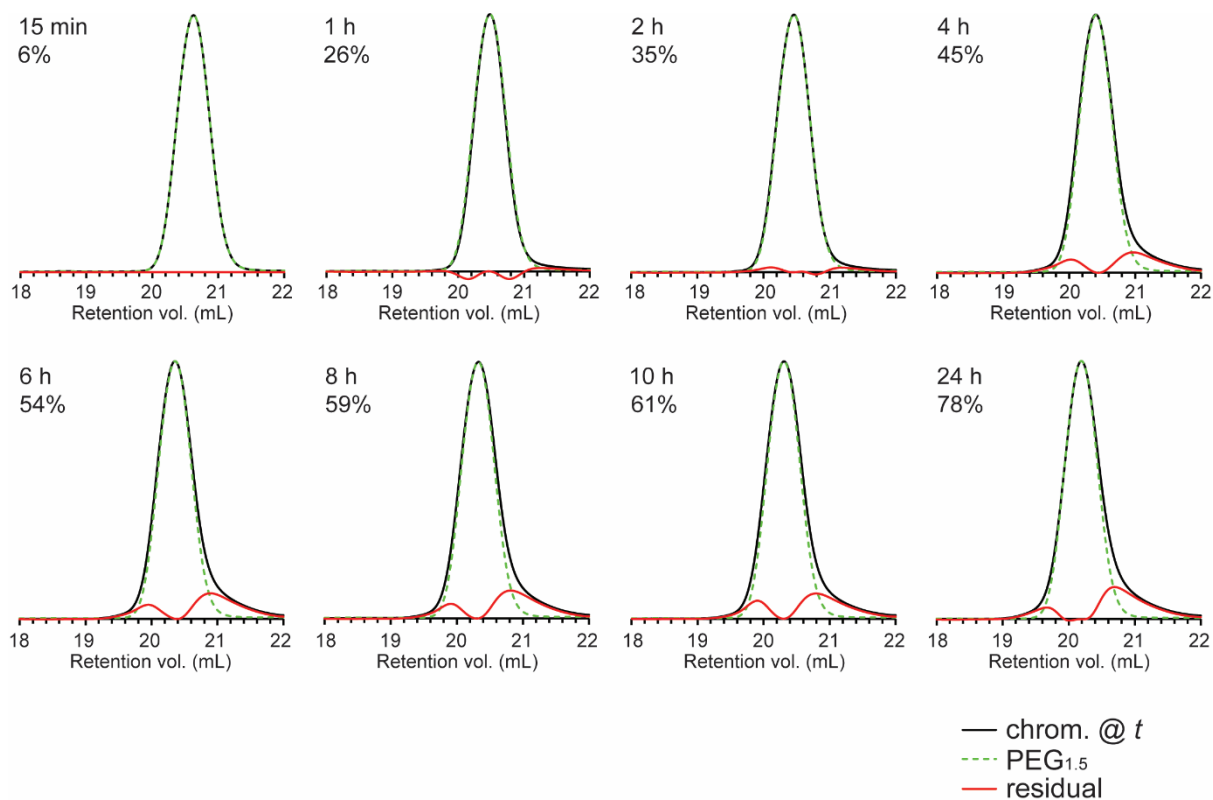


Figure S29. GPC DRI chromatograms over time for catalysed polymerisation with 0.2 wt% Sn(Oct)₂ at 100 °C (solid black line) as compared to the initial peak shape (dashed grey line) and the resulting residual determination (solid red line). Total percentage monomer conversion at each time point is specified under the time.

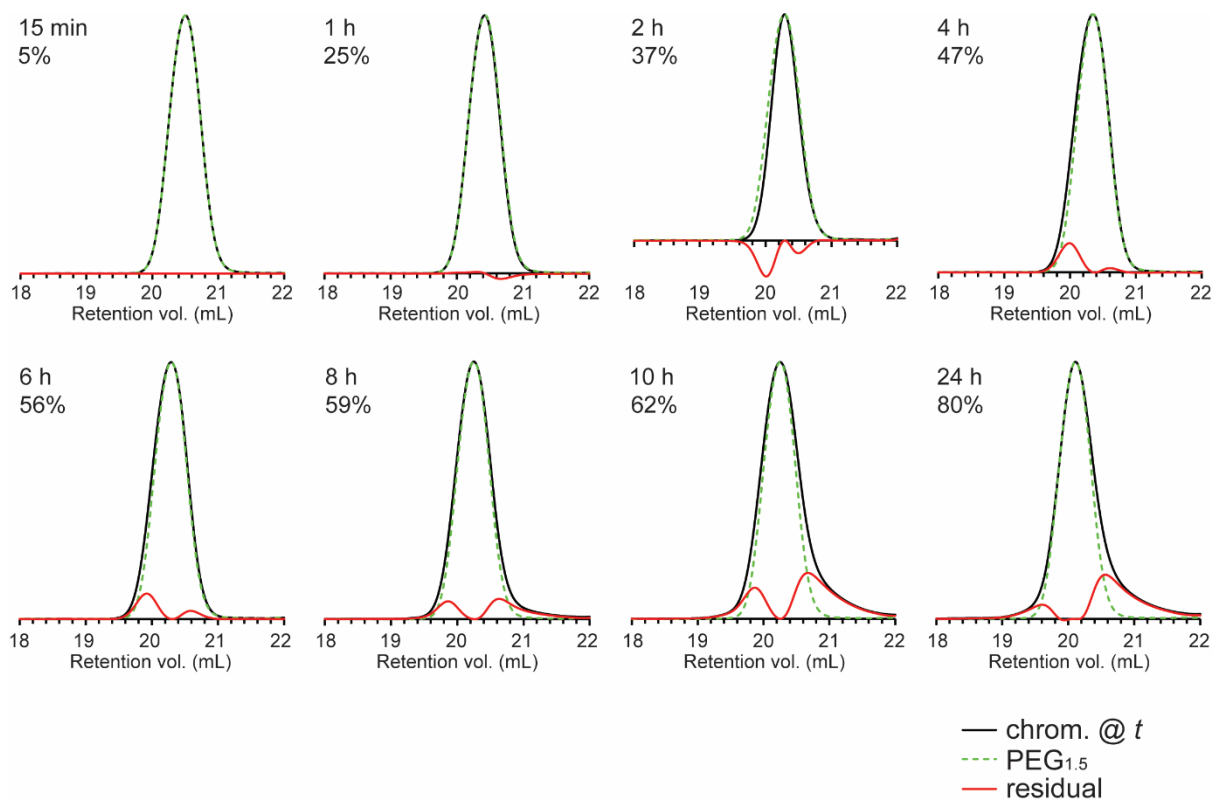


Figure S30. GPC DRI chromatograms over time for catalysed polymerisation with 0.4 wt% Sn(Oct)₂ at 100 °C (solid black line) as compared to the initial peak shape (dashed grey line) and the resulting residual determination (solid red line). Total percentage monomer conversion at each time point is specified under the time.

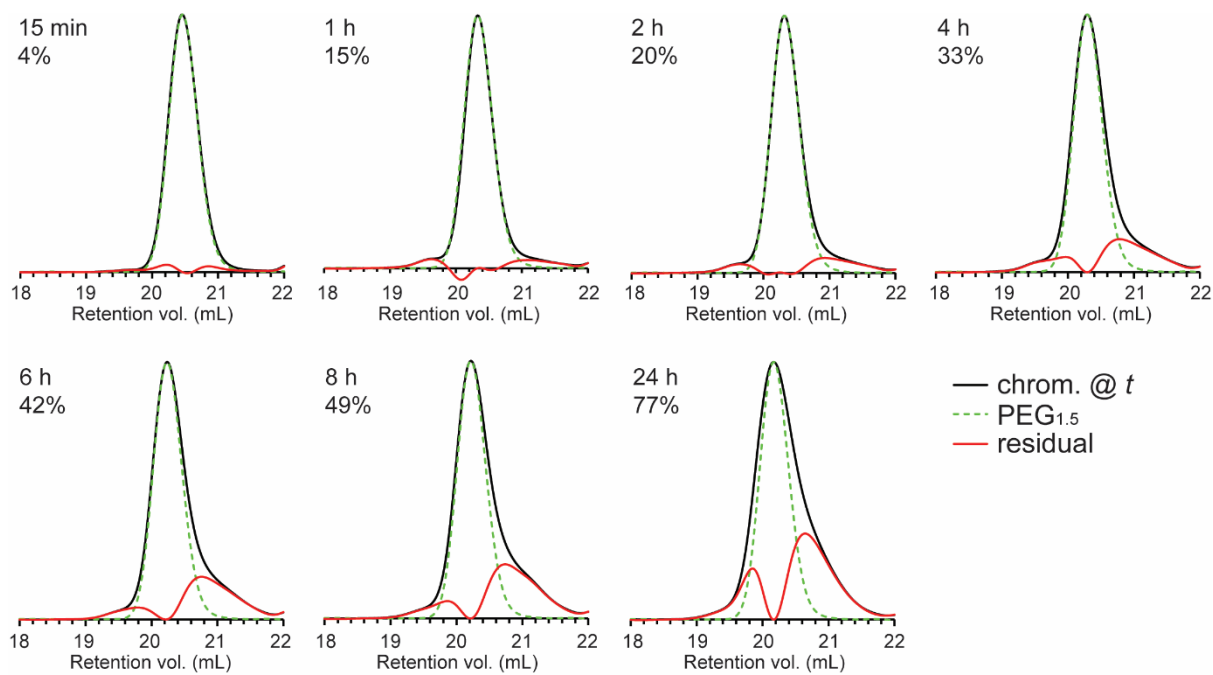


Figure S31. GPC DRI chromatograms over time for catalysed polymerisation with 0.1 wt% $\text{Sn}(\text{OTf})_2$ at 100 °C (solid black line) as compared to the initial peak shape (dashed grey line) and the resulting residual determination (solid red line). Total percentage monomer conversion at each time point is specified under the time.

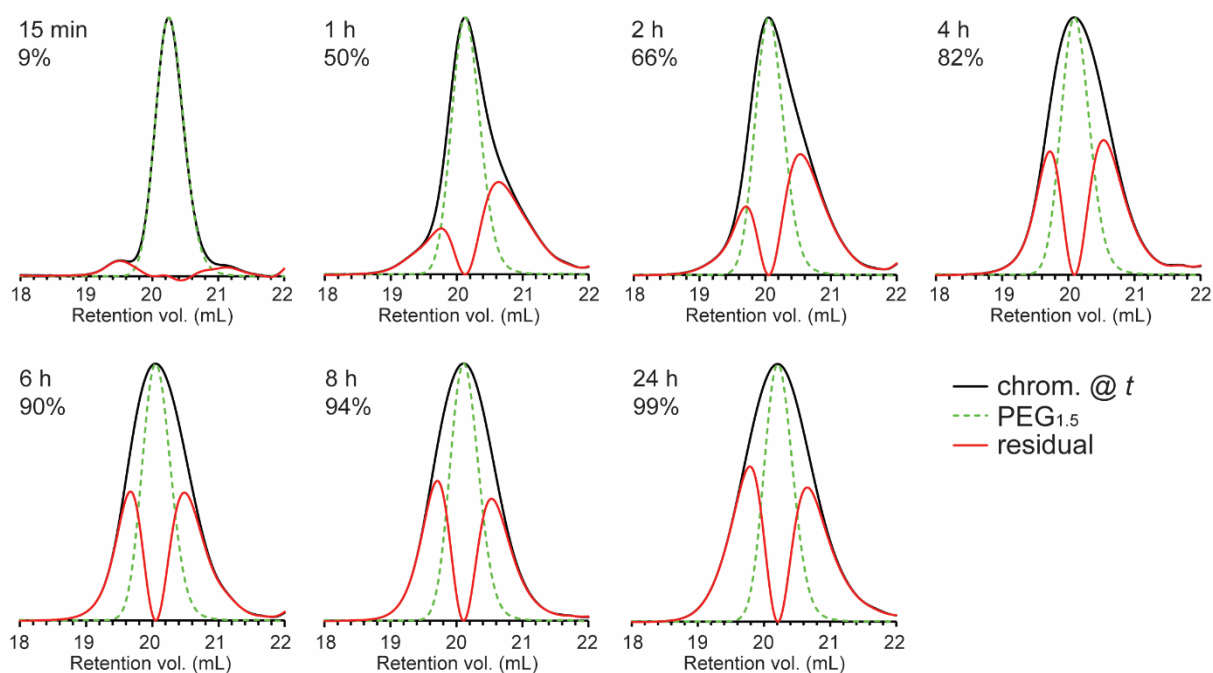


Figure S32. GPC DRI chromatograms over time for catalysed polymerisation with 0.4 wt% $\text{Sn}(\text{OTf})_2$ at 100 °C (solid black line) as compared to the initial peak shape (dashed grey line) and the resulting residual determination (solid red line). Total percentage monomer conversion at each time point is specified under the time.

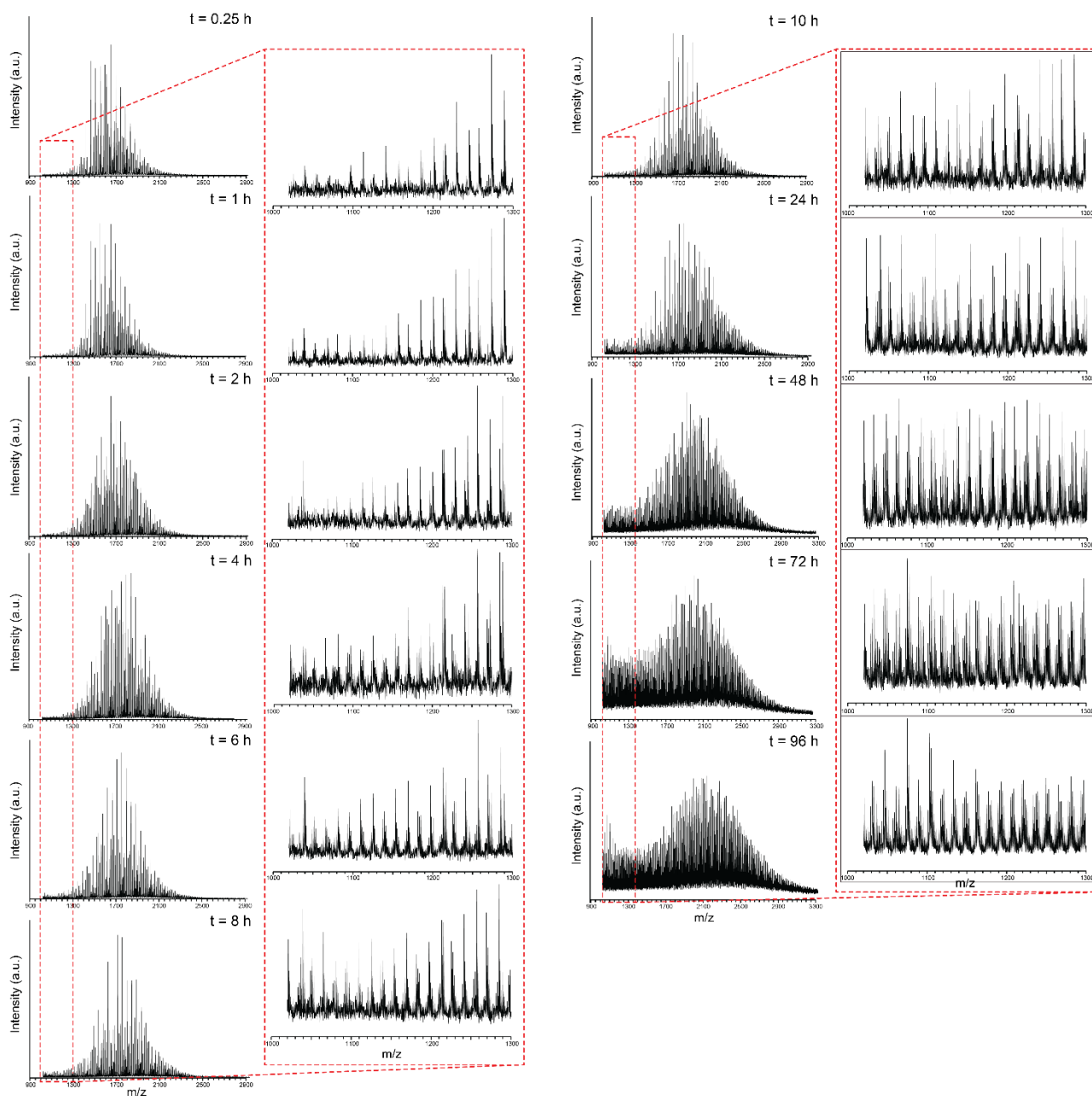


Figure S33. Matrix-assisted laser desorption/ionisation time-of-flight (MALDI ToF) mass spectra of the thermal polymerisation at 100 °C over time. Expansions show low m/z region.

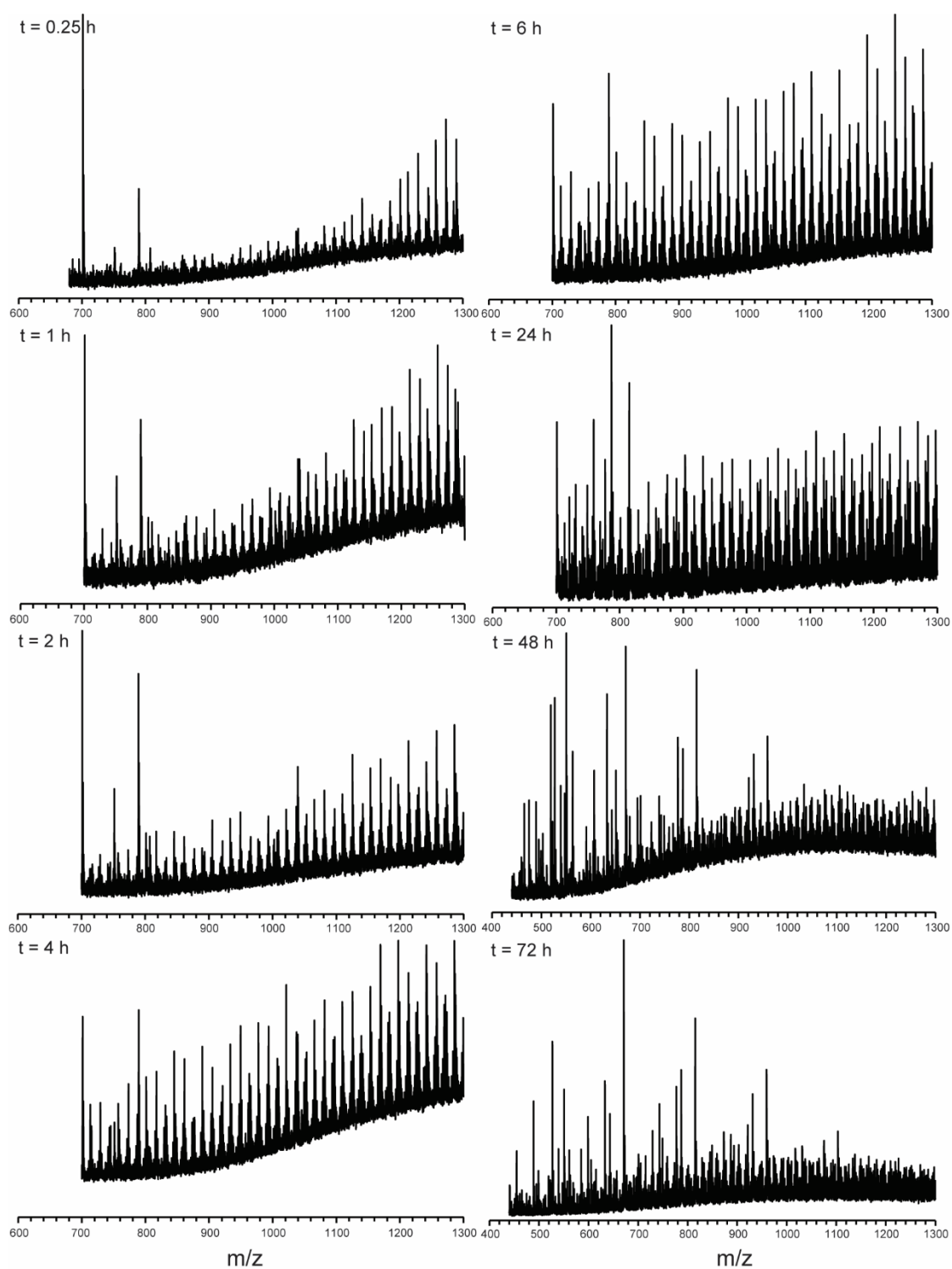


Figure S34. MALDI ToF mass spectra of the thermal polymerisation at 110 °C over time, showing the low m/z region.

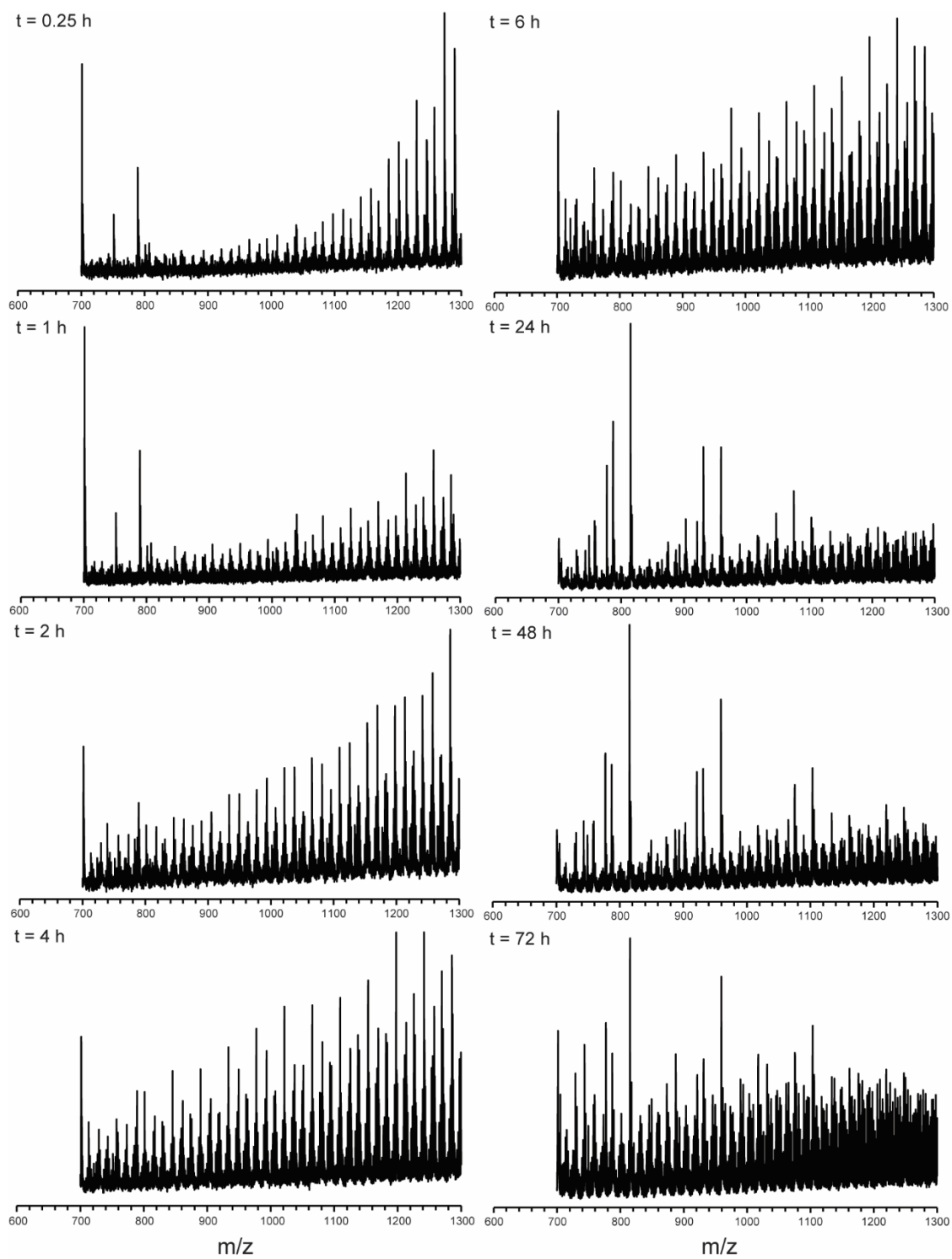


Figure S35. MALDI ToF mass spectra of the thermal polymerisation at 120 °C over time, showing the low m/z region.

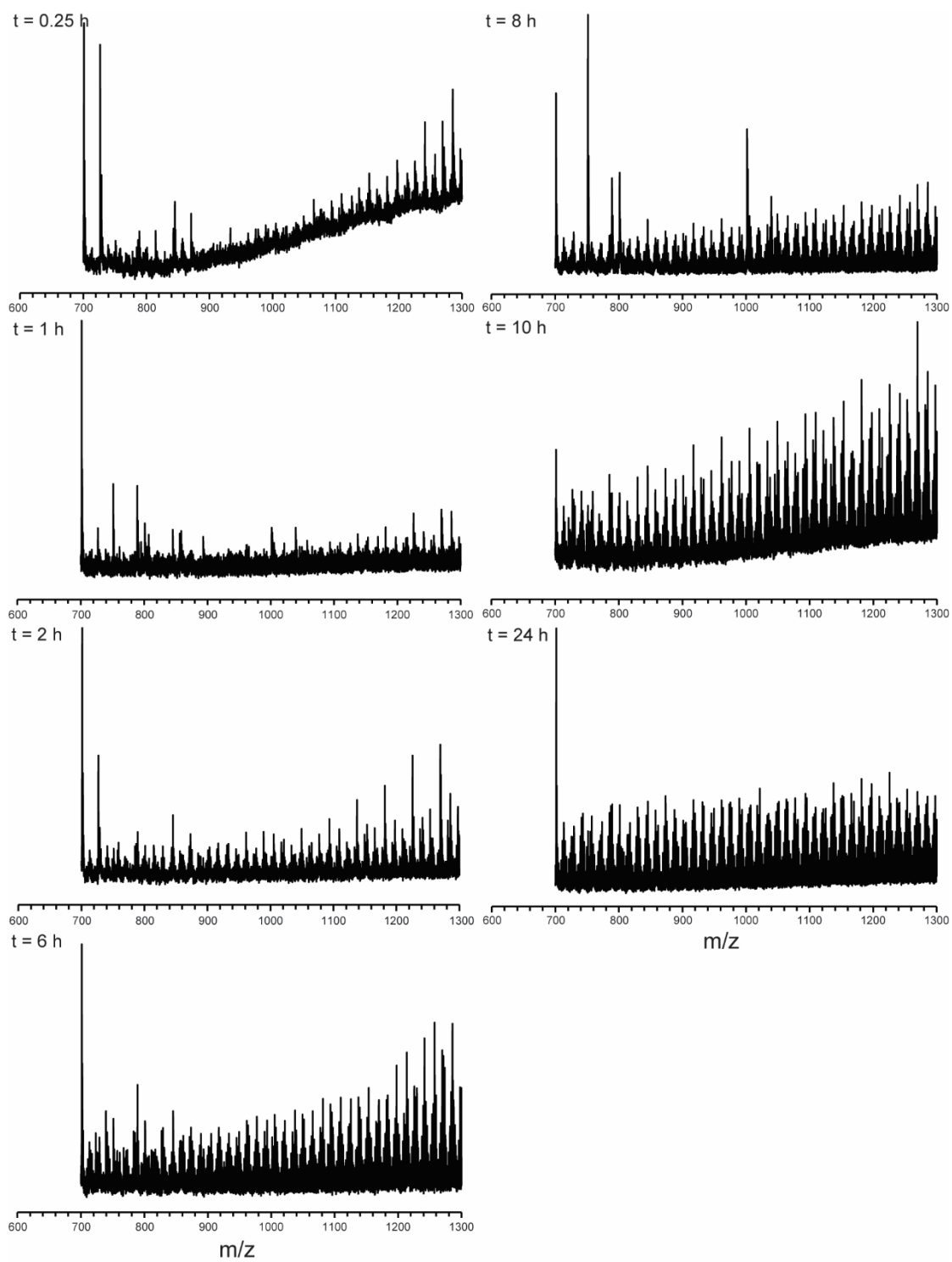


Figure S36. MALDI ToF mass spectra of the 0.1 wt% $\text{Sn}(\text{Oct})_2$ catalysed polymerisation at 100 °C over time, showing the low m/z region.

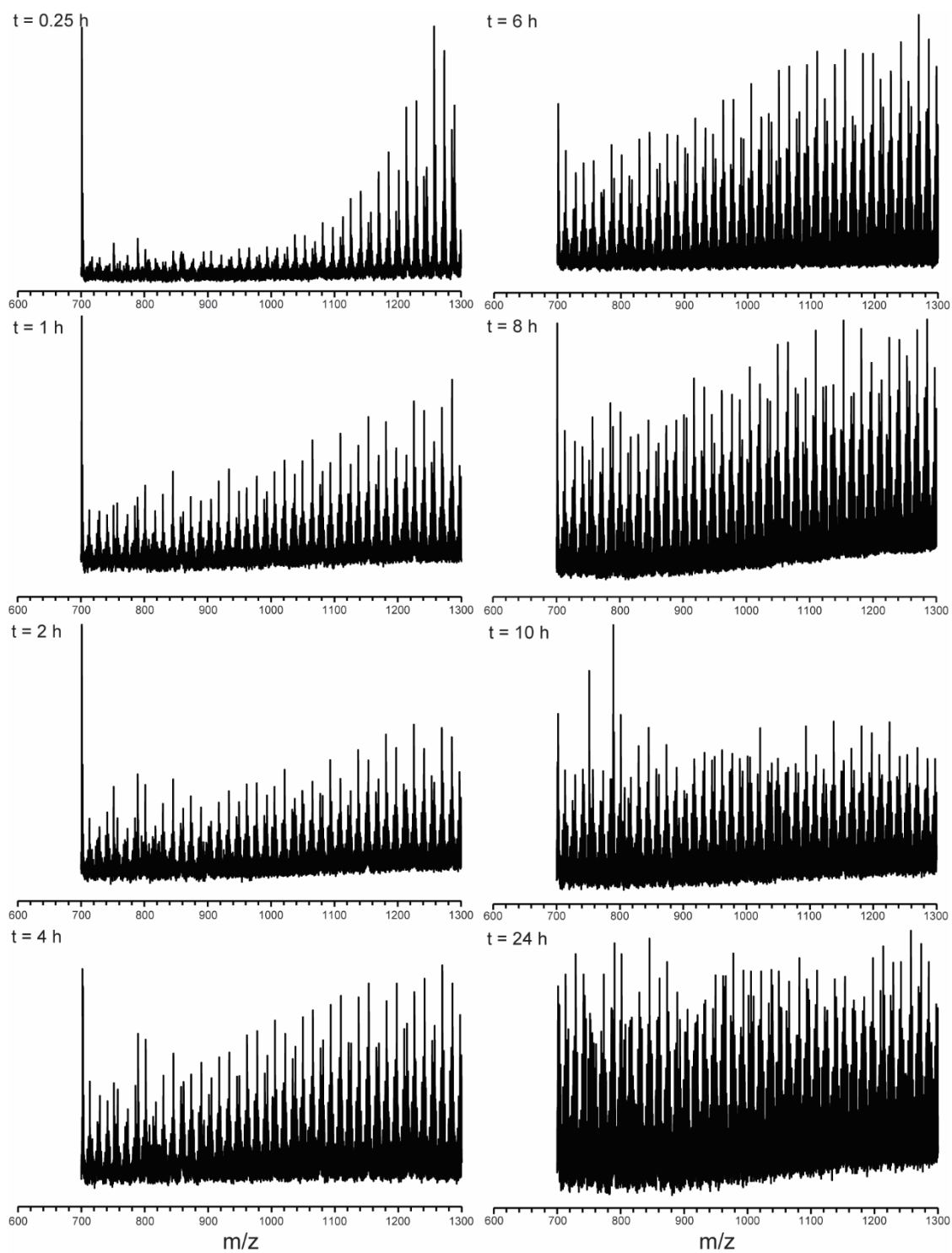


Figure S37. MALDI ToF mass spectra of the 0.2 wt% $\text{Sn}(\text{Oct})_2$ catalysed polymerisation at 100°C over time, showing the low m/z region.

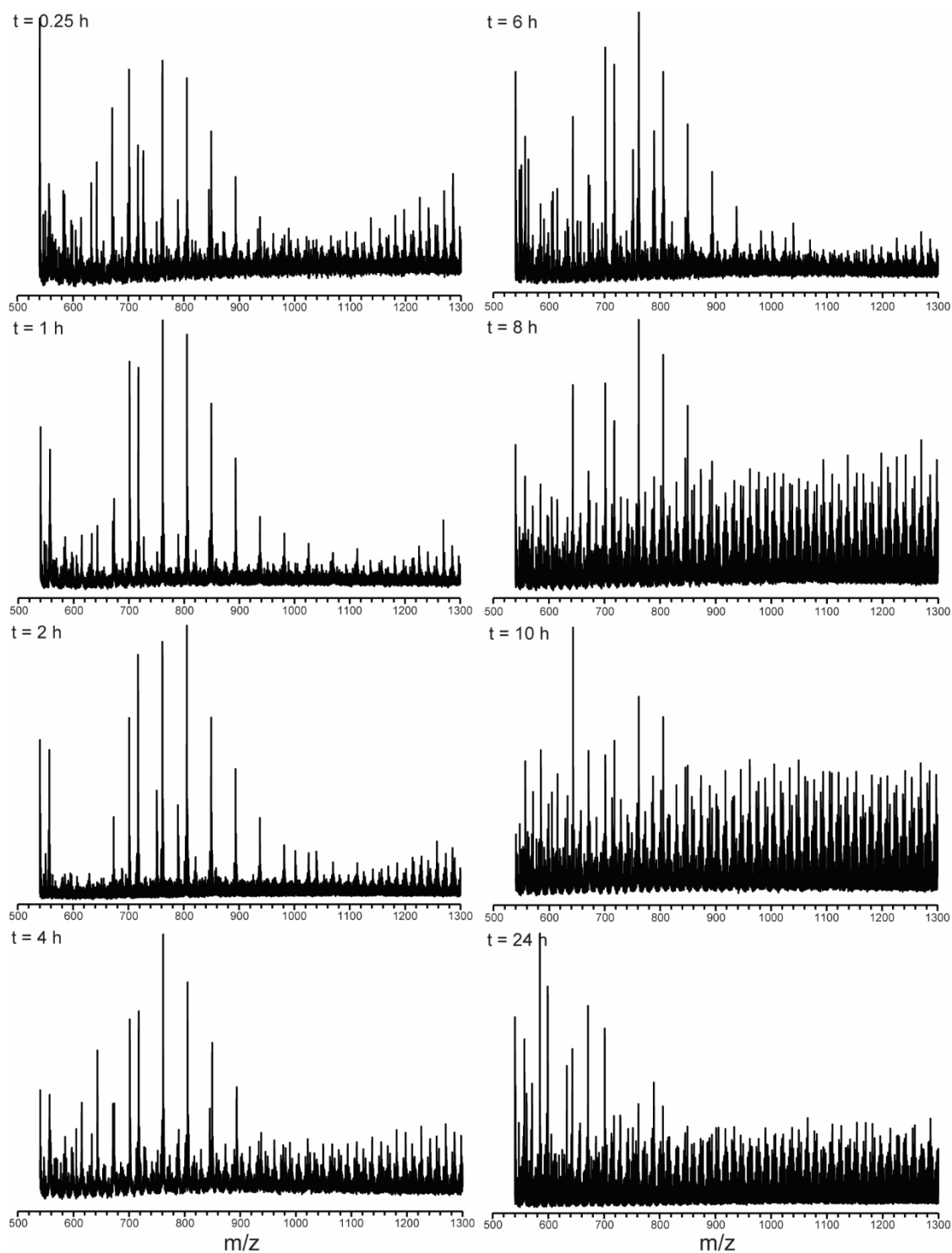


Figure S38. MALDI ToF mass spectra of the 0.4 wt% Sn(Oct)₂ catalysed polymerisation at 100 °C over time, showing the low *m/z* region. Contamination with PEG calibrants can be observed in some spectra as a repeating series separated by 44.03 *m/z* units between ~ 600–1000 *m/z*.

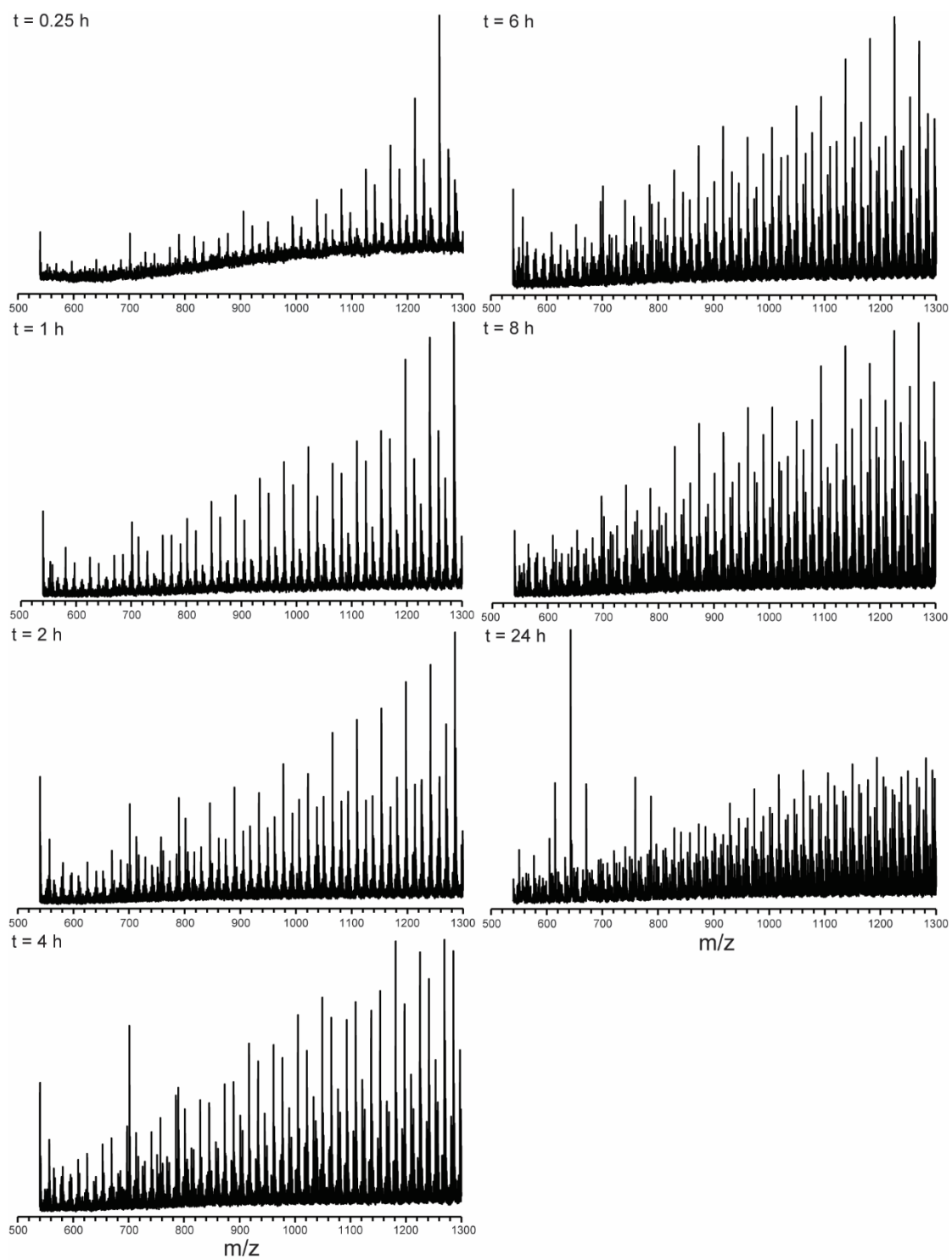


Figure S39. MALDI ToF mass spectra of the 0.1 wt% $\text{Sn}(\text{OTf})_2$ catalysed polymerisation at 100°C over time, showing the low m/z region.

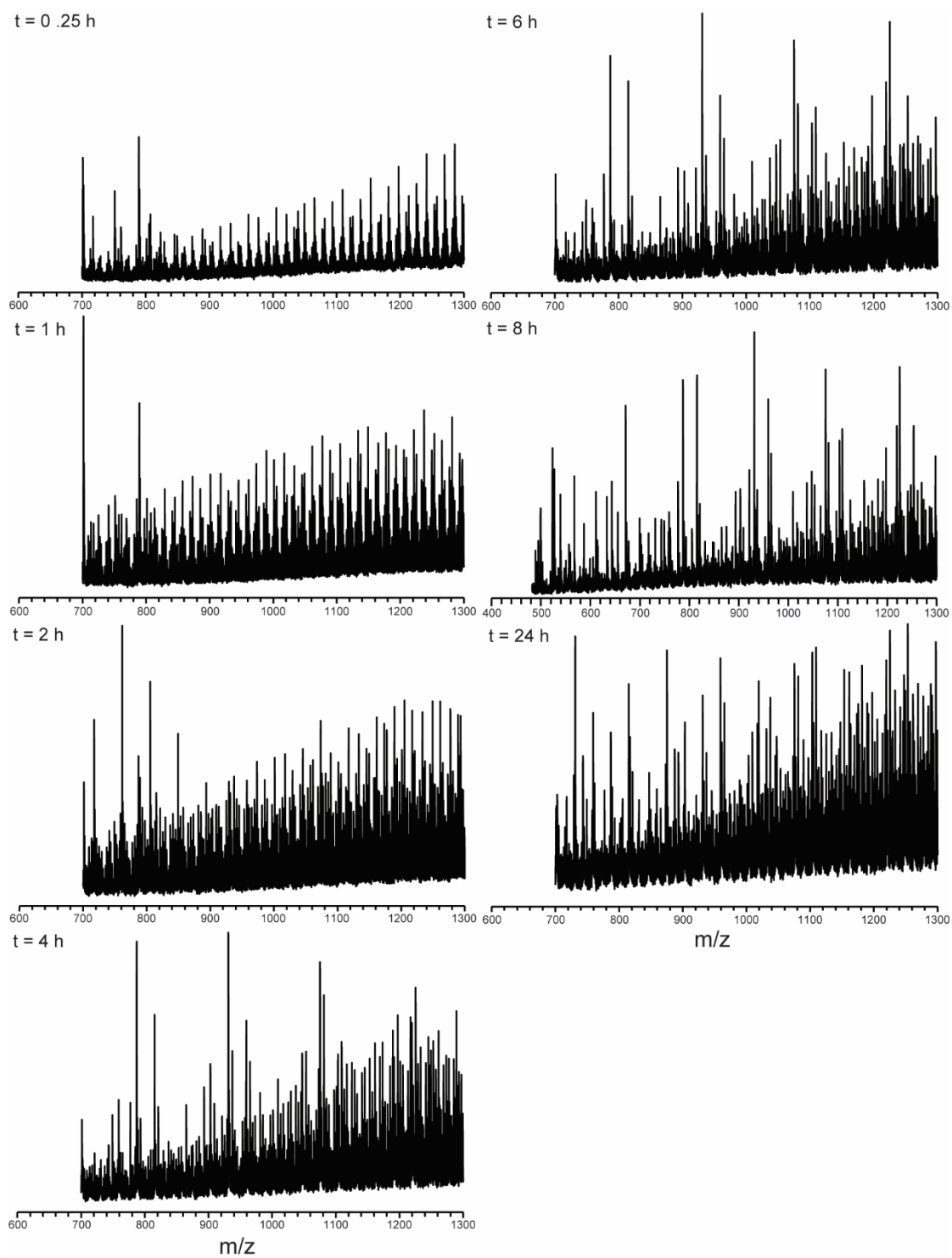


Figure S40. MALDI ToF mass spectra of the 0.4 wt% $\text{Sn}(\text{OTf})_2$ catalysed polymerisation at 100°C over time, showing the low m/z region.